Climate-driven water stress in the United States is seasonal, regional, and shaped by adaptation

Joey Blumberg[1*] and Travis Warziniack[1]

[1*]Rocky Mountain Research Station, USDA Forest Service, 240 W Prospect Rd, Fort Collins, 80526, CO, USA.

*Corresponding author(s). E-mail(s): joey.blumberg@gmail.com;
Contributing authors: travis.warziniack@usda.gov;

Abstract

This study quantifies drivers of US water use across the food-energy-water nexus and assesses how climate change, population growth, and adaptation may reshape future water scarcity. Using high frequency water withdrawal data from 2000–2020, we disentangle the effects of climate, hydrology, and socioeconomic factors on public water use (PU), crop irrigation (CI), and cooling for thermoelectric power generation (TP). Future water demands (2040–2070) are estimated using recent climate and socioeconomic projections, representing 1.0°C to 2.9°C warming and population growth ranging from 1% to 44%. Across 28 scenarios, we estimate annual water use changes ranging from -10.7% to +28.9% for PU, +32.1% to +43.6% for CI, and -27.9% to -19.9% for TP, contingent on continued adaptive efforts. Results reveal strong sectoral variation in climate sensitivity, seasonal mismatches between water supply and demand, and shifts in regional water stress under future warming.

Keywords: Water use, water scarcity, climate change, food-energy-water nexus

1 Introduction

Water scarcity is a pressing challenge worldwide, with billions of people relying on freshwater resources that are under mounting stress from climate change [1, 2], population growth [3], and unsustainable water use practices [4, 5]. In many regions, water supply systems depend on natural cycles of precipitation, snowmelt, and runoff, which regulate water availability for municipal use, agriculture, and energy production [6]. However, shifting climates are disrupting these cycles, leading to increasingly volatile water supplies [7–10]. Rising temperatures, altered precipitation patterns, and more frequent droughts are destabilizing freshwater resources, which have the potential for economic [11, 12], social [13–15], and environmental consequences [16–18].

Agricultural regions, particularly those dependent on seasonal snowmelt, face heightened risks of reduced crop yields and economic losses [19–23]. Energy sectors reliant on hydropower or water for cooling processes are similarly vulnerable [24–26]. In the United States (US)—a region with diverse climates and water needs—water scarcity is already a critical issue, particularly in the western US, where climate-driven water shortages are intensifying pressures across multiple sectors [24, 27–29]. Ongoing negotiations over Colorado River allocations have led to mandated water use reductions across multiple states [30], while the increasing frequency of snow drought conditions in the western US has reduced available water supplies [31]. Notably, during the 2026 water year, severe snow drought conditions were widespread across the western US. SNOTEL stations in every western state recorded record-low snow water equivalent, with large shares of monitoring sites classified in snow drought, including 95% in Colorado and over 80% in several other states [32]. At the same time, emerging evidence suggests that regions historically considered water-abundant, including parts of the eastern US, are also experiencing increasing drought risk [33]. Understanding these vulnerabilities, and designing effective solutions, necessitates disentangling the underlying drivers of water use, which emerge from both the natural environment and human responses.

Conceptually, water use reflects a combination of supply-side constraints and demand-side factors shaped by climatic, hydrologic, demographic, and institutional contexts [5, 9, 34–38]. Existing approaches to projecting water scarcity generally fall into two broad categories. Process-based and mass-balance models are well-suited for simulating hydrologic and biophysical processes but either omit human behavior or incorporate it through stylized or ad hoc assumptions (e.g., [22, 39, 40]). Integrated assessment models (IAMs), such as the Global Change Analysis Model (GCAM), embed these physical systems within partial equilibrium frameworks that represent interactions across energy, water, land, and economic systems under alternative policy and socioeconomic scenarios [41–44]. While IAMs capture important cross-sectoral feedbacks, behavioral responses in these models are

governed by structural assumptions and calibrated parameters, which can constrain how adaptation and decision-making are represented.

By contrast, we leverage newly available, high-frequency, spatially disaggregated water use data to provide an empirical assessment of the drivers of water use and water scarcity across the conterminous US (CONUS). By integrating these data with high-resolution climate and hydrologic information, we employ a reduced-form statistical approach to identify how water use responds to hydroclimatic and demographic variation. This approach captures historically revealed behavioral responses and adaptation without imposing structural assumptions about decision-making. We analyze combined surface and groundwater withdrawals across three sectors spanning the food–energy–water nexus: public use (PU), crop irrigation (CI), and thermoelectric power generation (TP), which together account for approximately 90% of total water withdrawals in the US [45].

We make three primary contributions. First, we provide regional-, seasonal-, and sector-specific estimates of how water use responds to climatic, hydrologic, and demographic drivers across CONUS. These empirically derived relationships offer a data-driven complement to existing modeling approaches and can inform both policy design and the behavioral assumptions embedded in IAMs. Second, we apply these estimated relationships to downscaled CMIP6 projections and a calibrated hydrologic model to project future water demand under diverse climate–population pathways, while accounting for structural changes in the energy sector through state-level transitions away from water-intensive thermoelectric generation [46]. Third, we integrate projected water demand with changes in water availability to identify regions where emerging imbalances between supply and demand are most likely to intensify water scarcity. Together, this framework links empirically grounded behavioral responses with projected changes in the human and natural environment, providing spatially explicit insights into future water scarcity risks in the coming decades (2040–2070).

2 Results and Discussion

2.1 Historical determinants of water use

The statistical models developed in this study reveal clear seasonality in the marginal responses of water use to hydroclimatic conditions across all sectors, as demonstrated in Figure 1, with seasonal patterns in water use and key climatic variables presented in Figure A1 and Figure A2. The marginal effects of temperature (1A, 1E, 1I), precipitation (1B, 1F), runoff (1C, 1G), and soil moisture (1D, 1H) vary substantially across months, with the greatest sensitivity observed during the warm season months (April to September). For example, the response of water withdrawals for CI to higher temperatures is strongest early in the planting season (May and June) when young plants are more sensitive to heat and water stress [47]. A 1°C increase in the average maximum temperature in June

is significantly correlated with a 27 acre-foot increase in water withdrawals for irrigation (1E), which is a 15% increase from the historical county average (2000-2020). The estimated marginal effects of precipitation (1F) and soil moisture (1H) in the same month indicate an inverse relationship, as wetter conditions reduce the need for irrigation. These patterns are qualitatively similar across most farm resource regions (defined by county clusters that share similar agricultural practices, farm characteristics, topography, climate, and other factors relevant to farming [48]), with differing levels of magnitude (see Figure A3).

Seasonal effects for PU display the same directionality (1A-1C), however the responses are more muted, where a 1°C increase in June drives a 3.7 gallon per person increase in withdrawals (+3.1%). Responses to changes in soil moisture (1D) display no clear seasonality with effects close to zero in magnitude. For TP, water withdrawals for cooling are positively correlated with energy demands, so warmer temperatures in winter months result in *lower* water withdrawals due to reduced household heating demands, and warmer temperatures in summer result in higher withdrawals (1I). It is also important to note that water withdrawals for power plants with recirculating cooling technologies exhibit lower sensitivity to temperature compared to those with once-through systems (see Figure A4). In general, our statistical models appear to capture the relationship between climate and water use in an intuitive manner.

After controlling for climate, hydrology, population, time-invariant county characteristics, and state-year specific shocks, we examine the linear trends that explain the remaining variation in water use for every county. We use these trends as an *ex post* assessment of the net effect of all water management policies, technological advancement, and behavioral changes within a county that may increase or decrease water use over time but are not directly observable. The slopes of these trends are displayed in Figure 2 with significant trends (at the 95% level) shown in Figure A5. For PU withdrawals (2A), most counties exhibit modest decreases in water use over time, consistent with reports from federal US agencies [45], with 60% of all counties displaying a 0 to 3 gallon per person annual decrease. This result is potentially attributable to efficiency gains in household appliances and a changing composition of the US economy to less water-intensive commercial enterprises [35, 49]. However, for CI (2B), the trends are much more varied. First, trends are much more pronounced in the western US, where irrigated agriculture is more prevalent. Counties in eastern Colorado, parts of California's Central Valley, and above the Ogallala Aquifer in Nebraska display decreasing water use trends, which may reflect recent responses to reduced surface water availability [38] and efforts to reduce groundwater pumping [50, 51]. Alternatively, pronounced increases in irrigation withdrawals are observed in parts of the Snake River Basin spanning southern Idaho and adjacent regions of Oregon and Nevada, where groundwater pumping has been shown to be unsustainable under historical management conditions [52]. In the wetter, eastern US, many counties display modestly increasing

irrigation water use. Producers in these areas have begun to adopt irrigation as an adaptation strategy to growing temperature variability and occasional droughts, as demonstrated by observed increases in irrigated cropland in Georgia, South Carolina, and areas along the Mississippi River Delta [53].

Adaptation to climate change and population growth can manifest in two ways: (1) reducing or increasing overall water use (as captured by time trends) and (2) dampening the marginal effects of climatic factors. For example, improvements in irrigation efficiency may lower total water withdrawals while simultaneously reducing the responsiveness of withdrawals to temperature changes. To test this, we allow the monthly effects of climate variables to vary by half-decade (see Equation 5) to assess whether water withdrawals have become more or less sensitive to fluctuations in temperature over the study period. Across all sectors, we find no statistically significant differences in the seasonal marginal effects of temperature across half-decade intervals (Figure A6). However, we do find suggestive evidence that withdrawals for PU may be growing less sensitive to temperature over time. For instance, a 1°C increase in June and July led to a 4.3 and 3.3 gallon per person increase in withdrawals, respectively, during the 2000–2004 period. By 2015–2019, these effects declined to 4.0 and 2.9 gallons, with proportional decreases observed across the intermediate half-decade intervals. Conversely, for CI and TP, the marginal effects of temperature modestly *increase* over the study period. For CI, this pattern may reflect nonlinear increases in atmospheric water demand at higher temperatures, which can amplify the marginal effect of additional warming, as baseline temperatures have risen over the study period.

2.2 Projected changes to water demands

To examine how water use responds to future climate and population trajectories, we focus on five stylized scenarios selected to span the range of projected warming, hydrologic change, and population growth. These scenarios correspond to representative GCM–SSP combinations capturing the coolest, hottest, driest, wettest, and a central ("Moderate") projection (Figure 3). Average underlying climate and population forcings for each scenario are summarized in Figure 4, which shows monthly changes in key hydroclimatic variables and the distribution of projected population growth across counties; corresponding county-level spatial patterns are presented in Figure A7.

Figure 5 decomposes projected changes in water withdrawals into contributions from climate, population growth, and long-run trends for the 2040–2070 period relative to 2000–2020. Panels (A)–(C) show monthly withdrawal responses to climate change across scenarios, panels (D)–(F) display annual changes attributable to population growth, and panels (G)–(H) present the distribution of county-level time trends. Climate-driven responses exhibit strong seasonality across all sectors (Figure 5A–C). For PU and TP, the magnitude of projected changes follows a clear temperature gradient, with warmer scenarios producing larger increases in withdrawals during summer months and

larger reductions during cooler months. In contrast, CI responses reflect a more complex interaction between temperature and moisture conditions. In particular, the *Warm and very dry* scenario produces increases comparable to the *Hot* scenario despite 1.4°C lower warming, highlighting how drier conditions affect irrigation demand.

Population-driven changes are more uniform (Figure 5D–F). Increases in PU withdrawals scale directly with projected population growth across scenarios. Effects for CI are comparatively small and centered near zero, while TP responses are positive but statistically imprecise, potentially reflecting limitations in linking plant-level water use to spatially aggregated populations in the supported grid. In terms of trends, they are predominantly negative for PU (Figure 5G), consistent with ongoing efficiency improvements. For CI (Figure 5I), the distribution of trends is centered near zero with a modest leftward shift but a pronounced right tail, indicating that while many counties exhibit stable or declining withdrawals, a subset experience substantial increases.

Aggregating county-level projections nationally, we estimate annual changes in sectoral water use of -10.7% to +28.9% for PU, +32.1% to +43.6% for CI, and -27.9% to -19.9% for TP across all 28 scenarios (with seasonal changes displayed in Figure A8). When summed across all sectors, projected changes in annual withdrawals range from -0.01% to +10.7%. While these national-level changes may appear modest, it is important to note that they are contingent on two critical assumptions: (1) historical adaptation efforts, as proxied by linear time trends, will continue at their observed rates; and (2) all 24 states with renewable energy plans will successfully meet their clean energy goals by 2050. These assumptions are relaxed and examined in the following section.

Projected changes in runoff and withdrawals reveal a pronounced seasonal divergence between water supply and demand under future climate conditions (Figure 6), highlighting challenges for intra-annual reservoir management. Winter runoff increases across all scenarios, rising by approximately 10% to 30% relative to the historical period, consistent with earlier snowmelt and a shift from snowfall to rainfall (Figure 6A), while runoff during late spring through early fall declines in most scenarios, falling by roughly 5%–20% in the driest cases. Changes in withdrawals exhibit an opposing seasonal pattern (Figure 6B). Withdrawals decline slightly during winter months, partly due to reduced thermoelectric cooling needs, but increase substantially during the warm season, with peak gains of approximately 10% to 25% in late spring and summer. These opposing trends are reflected in the net difference between runoff and withdrawals (Figure 6C). Winter months exhibit improvements in excess supply, while summer and early fall show consistent declines, with net water availability decreasing by up to 10%–25% across scenarios. Overall, these results highlight a growing temporal mismatch between peak water availability and peak demand, underscoring the importance of reservoir strategies that capture surplus winter runoff to buffer against intensifying summer shortages.

2.3 Water scarcity hot spots

While water withdrawals are largely projected to increase in aggregate across CONUS, future levels of water stress exhibit substantial geographic variation. A withdrawal-to-availability (WTA) ratio is used to identify watersheds in the US that may be vulnerable to future water scarcity. The WTA ratio highlights areas where local surface and subsurface (shallow groundwater) water resources can or cannot meet water demands. By comparing changes in WTA from the historical period (Figure 7A) to projected future scenarios (Figure 7B–F), we identify regions where water scarcity is either improving or worsening (corresponding changes in WTA magnitudes, projected stress levels, and counts of watersheds transitioning across stress categories are provided in Figure A9). A low water stress level indicates sustainable water use, a moderate level signals emerging water scarcity, and high to extreme levels represent intense water scarcity, where significant reliance on nonrenewable or nonlocal water sources is required.

One key observation is that the eastern US shows relatively little change in water stress levels across scenarios (Figure 7B–F), even under the warmest and driest conditions. Despite projected increases in demand driven by rising temperatures (Figure 1E) and positive trends in crop irrigation (Figure 2B), most watersheds in the eastern US remain in the same stress categories as the 2000–2020 period. This stability suggests that relatively abundant water resources can accommodate increased demand without triggering widespread shifts in water scarcity. Patterns in the western US are more nuanced and highly scenario-dependent. In particular, the dry scenarios (Figure 7B–C) produce more widespread increases in water stress than the *Hot* scenario (Figure 7F), even though they feature 1.4–2°C less warming and substantially lower population growth (Figure 4E). This pattern suggests that mitigating future water scarcity requires both supply- and demand-side approaches. Consistent increases in water stress are observed in parts of the northern and interior West (including the Dakotas, Montana, and Wyoming) where multiple scenarios show transitions from low to moderate or higher stress levels. Additionally, the southern Great Plains (Texas, Oklahoma, and Kansas) exhibit notably adverse conditions under the drier scenarios.

Interestingly, several regions in the Southwest (Southern California, New Mexico, and Southern Arizona) exhibit consistent *improvements* in water stress under scenarios that are not moisture-limited (Figure 7D–E). These improvements are largely attributable to the continuation of historical declines in water use (Figure 2B), which offset the effects of future climate and population growth. However, these gains should be interpreted cautiously. Although some watersheds transition to lower stress categories (e.g., from extreme to severe or from severe to very high), most remain at or above high water stress across scenarios, indicating that current rates of adaptation are insufficient to achieve sustainable water use in the near future. More broadly, while these trends indicate some

degree of resilience, they are unlikely to fully mitigate future water scarcity risks without more substantial changes in water management and policy.

2.4 Policy implications

The spatial patterns in projected water scarcity highlight where vulnerabilities emerge under future climate and population pressures, but they do not indicate which interventions are most effective at mitigating these risks. To address this, we implement a set of counterfactual policy and demand reduction scenarios that isolate the effects of key adaptation pathways, including improvements in irrigation efficiency and shifts toward less water-intensive thermoelectric cooling technologies (Figure 8C–E). These scenarios, described in Section 4.6, are designed to reflect ongoing policy discussions and investments in water-saving technologies across the US, such as federal programs promoting irrigation efficiency (e.g., [54]) and regulatory efforts to reduce cooling water withdrawals in the power sector (e.g., [55]). We also include a "no adaptation" scenario that removes estimated trends and state-level renewable energy transitions to evaluate how reversals or delays in policy implementation (e.g., [56]) may affect future scarcity (Figure 8F). By comparing these counterfactuals to the *Moderate* scenario baseline, we assess both the magnitude and spatial distribution of potential gains from targeted interventions, as well as the losses associated with their absence.

Across sectors, efficiency improvements unsurprisingly reduce water use, although the magnitude and distribution of these effects vary by sector (see Figure A10). Improvements in TP cooling produce the largest within-sector reductions, compressing changes in withdrawals toward zero across most counties, while improved CI efficiency primarily reduces the upper tail of large increases in demand. The no adaptation counterfactual shifts withdrawals upward across nearly all counties for both PU and TP. CI responses remain more heterogeneous, with both the no adaptation and efficiency scenarios dampening large increases while increasing the mass near zero, indicating that these effects are concentrated in counties experiencing the greatest expansions in irrigation demand.

These sectoral differences translate into distinct spatial patterns in water scarcity (Figure 8). Improvements in CI efficiency yield the most geographically concentrated benefits, particularly in the northern and interior West (parts of the Dakotas, Montana, and Idaho) where they prevent transitions into higher stress categories (Figure 8C). Improvements in TP efficiency produce more limited and spatially diffuse effects (Figure 8D), reflecting the concentration of thermoelectric generation in relatively water-abundant regions of the eastern US. When combined (Figure 8E), these efficiency gains produce broader, but still uneven, reductions in water stress. By contrast, removing adaptation reverses most of the improvements present in the baseline scenario. Under this no adaptation scenario (Figure 8F), water use increases across most regions, and previously observed improvements

in the Southwest are largely eliminated. Overall, these patterns highlight the extent to which projected reductions in water stress depend on the continuation of recent efficiency gains and structural transitions, as well as the efficacy of different policy pathways aimed at achieving sustainable water use.

3 Conclusion

This paper provides a comprehensive analysis of water use patterns in the US and projects future water demand under multiple climate and socioeconomic scenarios. We further evaluate a set of counterfactual policy scenarios to isolate the effects of key adaptation pathways. To our knowledge, this is the first study to explain and forecast spatially-disaggregated water use at the CONUS scale using a reduced-form statistical approach, while also accounting for human behavior. To that end, we offer four key insights for policymakers seeking to design targeted, region-specific interventions to mitigate future water scarcity.

First, future water use will be shaped by opposing forces: increases in withdrawals driven by climate change and population growth, particularly during warm-season months, and decreases in withdrawals from continued adaptation efforts, such as improved efficiency in domestic water use and renewable energy plans that reduce reliance on water-intensive power generation. Rising temperatures and shifting hydrology are projected to increase water withdrawals, particularly for irrigation, with total US water use ranging from -0.01% and 10.7% by 2070, depending on the scenario. Second, we highlight pronounced seasonal divergence between water supply and demand. Summer months will see amplified peaks in withdrawals due to increased evaporative demands for irrigation and public use. Conversely, winter withdrawals are expected to decrease because lower heating demand reduces the amount of water required for thermoelectric power generation. These seasonal variations have important implications for water management and infrastructure planning, as the intra-annual timing of peak demands may coincide with lower water availability due to shifting hydrological cycles and earlier runoff. Third, we identify critical geographic hot spots of future water scarcity within the US. While areas like Arizona, southern California, and New Mexico may see modest improvements in water stress due to continued adaptation efforts, they will remain heavily reliant on nonlocal transfers and groundwater. Regions such as Texas, Montana, and the Dakotas are projected to experience significant increases in water stress across multiple scenarios, underscoring the need for targeted, region-specific management strategies. Lastly, our counterfactual analysis shows that improved irrigation efficiency is most effective in the northern and interior West, where it prevents future transitions into higher water stress categories, while thermoelectric efficiency yields more diffuse and comparatively modest benefits at the basin scale. Overall, these results highlight that policy effectiveness varies substantially across sectors and regions.

Several limitations should be considered when interpreting these results. First, our projections rely on historically observed relationships over 2000–2020 and do not explicitly account for emerging sources of water demand, such as the rapid expansion of water-intensive data centers [57] or proposed increases in nuclear power infrastructure [58]. These sectors may represent important drivers of future water use that are not captured in our analysis. Second, while our modeling framework incorporates adaptation through estimated time trends and policy-informed energy transitions, it does not explicitly model future technological innovation, structural economic change, or future global food demand that may affect irrigation water use. We also acknowledge potential endogeneity concerns within our statistical framework, arising from interactions across water use sectors and institutional allocation mechanisms. While our empirical strategy addresses some of these concerns, some interdependencies across water use sectors may not be fully captured. These limitations are discussed further in Sections 4.2.5 and 4.7.

In conclusion, this study offers a scalable framework for evaluating water use trends and scarcity risks, and guiding water management strategies. With sufficient data, our approach can be extended to other contexts globally, providing actionable insights for water resource management under a changing climate.

4 Methods

4.1 Data preparation

To identify the key determinants of historical water use, we compiled a county-level panel dataset from 2000-2020 on water withdrawals, climate, hydrology, and population. We obtained data on combined surface and groundwater withdrawals from the USGS, which provides monthly data for public use [59] and crop irrigation [60] at the HUC12 scale from 2000-2020, and for plant-level thermoelectric power generation [61] from 2008-2020. Public water use refers to water that is withdrawn by public and private water suppliers for domestic, commercial, industrial, and other public water uses such as irrigation for parks. For crop irrigation, monthly irrigation withdrawals are estimated using reference evapotranspiration and crop-specific coefficients applied to annual crop classifications from the USDA Cropland Data Layer. Summary statistics for sector-level water use are available in Table A1. For climate and hydrology variables, we used historical monthly averages of weather from Daymet [62], paired with a calibrated Variable Inflation Capacity (VIC) model for estimates of surface and subsurface runoff, soil moisture, and snow-water equivalent [63]. The effects of human regulation and management are not captured in the VIC modeling framework, therefore surface runoff represents only naturalized (or unregulated) flow. Lastly, we used annual, county population data from

the Bureau of Economic Analysis [64]. For spatial consistency with the population data, water withdrawals for public use and crop irrigation were aggregated to the county-level using an area-weighted spatial average for HUC12 subbasins overlapping a county's border. Using the county as the unit of analysis is appropriate as many water management programs are administered at the county level.

To examine implications for future water use under a changing climate, we used projected climate, hydrology, and population data from seven GCMs and four SSP-RCP combinations for a total of 28 possible futures from 2040-2070. The narratives associated with the SSP-RCP scenarios can be summarized as:

- **SSP 1, RCP 2.6 (SSP126):** A sustainable world with strong global cooperation and low challenges to mitigation and adaptation, focused on reducing emissions,
- **SSP 2, RCP 4.5 (SSP245):** A "middle-of-the-road" scenario with moderate socio-economic growth trends and a balance between adaptation and mitigation efforts,
- **SSP 3, RCP 7.0 (SSP370):** A fragmented world with weak international cooperation, high emissions, and significant challenges to mitigation and adaptation,
- **SSP 5, RCP 8.5 (SSP585):** A fossil-fuel-driven world with rapid economic growth, high emissions, and a focus on adaptation over mitigation [65].

These scenarios encompass a range of assumptions regarding future climate responses and emissions trajectories, and the GCMs were chosen to ensure minimal overlap in their climate responses and modeling errors when representing historical climate in the conterminous US [66, 67]. The projected climate data were downscaled using the Double Bias Correction Constructed Analogs method [68], using Daymet as the meteorological reference dataset. The climate data were then used to drive the same calibrated VIC model used to generate the historical hydrology variables to project future hydrology under all scenarios [63]. Lastly, we used population projections downscaled to the county-level for each SSP [69]. These projections are estimated using an econometric model that accounts for historical county-level population trends and economic conditions, and they are downscaled from national SSP scenarios to reflect plausible local growth trajectories. A summary of data sources is available in Table A2.

In summary, across all counties in the conterminous United States, the 28 GCM–SSP combinations examined in this study capture average temperature increases of approximately 1.0°C to 2.9°C, soil moisture changes ranging from a decrease of 19 mm to an increase of 12 mm, and population growth between 1% and 44% by 2070. To aid interpretation while preserving the range of projected outcomes, we selected five stylized scenarios that span the joint distribution of climate and population change across the full ensemble. Specifically, we identified representative GCM–SSP

combinations corresponding to the coolest, hottest, driest, wettest, and a central ("Moderate") outcome in temperature–soil moisture space (Figure 3). These scenarios are labeled as: (1) Cool and dry, (2) Warm and very dry, (3) Moderate, (4) Warm and wet, and (5) Hot. Together, these scenarios capture the range of hydroclimatic and demographic conditions represented in the ensemble, while maintaining a tractable set of cases for analysis. The selected scenarios are further characterized by their seasonal climate and population forcings over 2040–2070 relative to the 2000–2020 baseline (Figure 4).

4.2 Modeling water use

To analyze the determinants of water use for PU, CI, and TP cooling, we employ three distinct econometric modeling strategies to best capture the data generating process for each sector.

4.2.1 Public use

For public use, we first calculated water withdrawals per capita (WPC^{PU}) by dividing total withdrawals (W^{PU}) by population (P) for each county-time step. We then estimated the following econometric model:

$$WPC_{it}^{\mathrm{PU}} = \sum_{j=1}^{12} \left[\mathbf{1}(m(t) = j) \times \mathbf{X}_{it} \boldsymbol{\beta}_j \right] + \theta_{i,m(t)} + \gamma_{s(i),t} + h_i(t) + \varepsilon_{it} \tag{1}$$

where WPC_{it}^{PU} represents average daily water withdrawals per capita for county i during time t (year-month) for PU, and $\mathbf{1}(m(t) = j)$ is an indicator function that takes the value 1 when the month of t is equal to month j, and 0 otherwise. $\mathbf{X}_{it}$ is a matrix of climate and hydrology variables (maximum temperature, precipitation, relative humidity, runoff, soil moisture, and wind speed) that interacts with the indicator function to capture seasonal effects, and $\boldsymbol{\beta}_j$ is the vector of month-specific parameters that were estimated. Allowing the impact of variables like temperature to vary by month is important because climate impacts on water demand and supply are likely heterogeneous across seasons. The term $\theta_{i,m(t)}$ is a county-month fixed effect that captures unobserved heterogeneity that is constant over time (for a given calendar month) but varies across counties, such as access to water markets. The term $\gamma_{s(i),t}$ is a state-by-year fixed effect, which controls for common shocks that affect all counties during year t within state s, such as abrupt changes in water pricing, policy mandates, or reservoir conditions. The term $h_i(t)$ represents a county-specific linear time trend. This trend is included to capture residual variation in water use that is not explained by observed climate, hydrology, or the high-dimensional fixed effects. While we do not directly observe changes in infrastructure, policy enforcement, or user behavior over time, the county-specific time trend serves as a flexible

proxy for these unmeasured, evolving factors. For instance, a negative trend may reflect improvements in conservation technology, shifts in pricing or policy, or behavioral adaptations that reduce demand—developments that are not explicitly captured in the dataset but nonetheless influence long-run patterns. Conversely, a flat or positive trend may indicate limited adaptation or countervailing pressures such as rising indoor demand. Importantly, we interpret $h_i(t)$ as a reduced-form summary of the net effect of all time-varying, county-specific factors—technological, institutional, behavioral, or otherwise—that influence water use beyond climate. The time trend also implicitly controls for the general rise in water prices over the study period, which have increased approximately linearly in many regions (see Figure A11). While the trends are included as a statistical control, they can also be evaluated *ex post* to examine whether their direction and magnitude align with known patterns of adaptation, conservation, or policy change.

Lastly, ε_{it} denotes the idiosyncratic error term. Standard errors are clustered in two dimensions: within counties and within state-by-year. Clustering within counties addresses the issue of autocorrelation within each county over time. This is critical because water use outcomes in a county are not isolated incidents and are likely influenced by past events and conditions, leading to a natural correlation in observations across different years within the same county. Clustering within state-by-years aims to account for the spatial correlation that may exist across different counties within the same state. Counties in a particular state are likely to experience similar policy environments, economic conditions, and climatic influences, leading to potential correlations in their economic outcomes. By simultaneously clustering standard errors in these two dimensions, this approach accounts for both the spatial dependencies across counties within a state and the temporal dependencies within each county [70, 71]. The model allows for a causal interpretation of the estimated parameters $\boldsymbol{\beta}_j$ under the assumption that all other factors influencing water use are either controlled for by fixed effects and time trends or captured by the error term [72].

4.2.2 Crop irrigation

For crop irrigation, agricultural water needs vary substantially based on both seasonal and geographic factors, including climate, soil types, and crop characteristics. To account for this heterogeneity, we incorporated information on the farm resource regions (FRRs) delineated by the Economic Research Service (ERS). These nine regions are based on county clusters that share similar agricultural practices, farm characteristics, topography, climate, and other factors relevant to farming [48]. The econometric model for CI was thus specified as:

$$W_{it}^{\mathrm{CI}} = \sum_{j=1}^{12} \sum_{r=1}^{R} \left[\mathbf{1}(m(t) = j) \times \mathbf{1}(FRR(i) = r) \times \mathbf{X}_{it} \boldsymbol{\beta}_{jr} \right] + \alpha P_{it} + \theta_{i,m(t)} + \gamma_{s(i),t} + h_i(t) + \varepsilon_{it} \quad (2)$$

where W_{it}^{CI} represents average daily water withdrawals for county i during time t (year-month) for CI, $\mathbf{1}(m(t) = j)$ is an indicator function that equals 1 when the month of t is j, and 0 otherwise, and $\mathbf{1}(FRR(i) = r)$ is an indicator function that equals 1 if county i belongs to FRR r, and 0 otherwise. The matrix $\mathbf{X}_{it}$ contains climate and hydrology variables which interact with the indicator functions to allow the coefficients in $\boldsymbol{\beta}_{jr}$ to vary across both months and regions. This double interaction captures the heterogeneous impacts of climate and hydrology on irrigation water use, accounting for variation in seasonal water demand and regional agricultural practices. We also controlled for population P_{it}, as there is evidence of agricultural land near fast-growing urban centers leaving production [73]. Similar to Equation 1, this model was also saturated with fixed effects and time trends to control for factors that we could not directly observe with available data. We also estimated a simplified version of Equation 2 that excludes the regional indicator function to visualize average effects of climate across the whole study sample.

4.2.3 Thermoelectric power generation

For thermoelectric power generation, we applied a different process for aggregating data given that the withdrawal data is plant-level and energy demands that drive withdrawals for cooling may not be driven solely by local populations and weather. In the US, electricity is managed and distributed through interconnected regional energy grids, overseen by Independent System Operators (ISOs). There are 10 ISOs in the conterminous US, and their role is to balance supply and demand across their territories to ensure grid stability and reliability while facilitating competitive wholesale electricity markets [74]. These markets set electricity prices based on real-time supply and demand conditions across the ISO region, influencing how power is dispatched from plants and shaping operational decisions, including water use for cooling.

While ISOs enable electricity to flow across state lines and regions, local conditions still exert meaningful influence on power plant operations. Transmission constraints, especially in areas with older infrastructure, can limit the ability of regional grids to efficiently transfer electricity during periods of high demand [75]. These constraints amplify the impact of localized climatic events, such as heat waves, which simultaneously increase energy demand for cooling and reduce the efficiency of electricity transmission. Heat waves also affect thermoelectric power generation directly, as elevated temperatures can reduce the efficiency of cooling systems and increase water withdrawal requirements to maintain operational capacity. As a result, even within interconnected grids, local climatic stressors can disproportionately affect nearby power plants, making localized climatic variables relevant for capturing water withdrawal dynamics.

To account for these nuances, we first construct annuli around each plant based on mean water withdrawals. Specifically, we assigned a maximum transmission constraint radius of 250 km for the

largest plant in terms of mean water withdrawals over the study period and scaled radii linearly downward for smaller plants.[1] The transmission constraint radius for each plant p was calculated as follows:

$$R_p = R_{\min} + \left(\frac{\bar{W}_p^{\mathrm{TP}} - W_{\min}^{\mathrm{TP}}}{W_{\max}^{\mathrm{TP}} - W_{\min}^{\mathrm{TP}}} \right) \times (R_{\max} - R_{\min}) \tag{3}$$

where R_p is the radius for plant p (in km), $R_{\min}$ is the minimum radius (50 km), $R_{\max}$ is the maximum radius (250 km), $\bar{W}_p^{\mathrm{TP}}$ is the mean water withdrawal of plant p (in MGD), and $W_{\min}^{\mathrm{TP}}$ and $W_{\max}^{\mathrm{TP}}$ are the minimum and maximum mean water withdrawal across all plants. Then, for each plant, climate variables such as temperature, humidity, and wind speed were averaged spatially across the defined annuli (see Figure A3).

We also leveraged information on the type of cooling system at a plant to allow for more heterogeneous impacts. Cooling systems in thermoelectric power plants differ in their water use and efficiency: once-through systems withdraw large volumes of water and return it to the source with minimal evaporation, recirculating systems reuse water through cooling towers but experience higher evaporation rates, and complex systems employ a combination of methods to optimize efficiency and water use based on local conditions. The econometric model was specified as follows:

$$W_{pt}^{\mathrm{TP}} = \sum_{j=1}^{12} \sum_{k=1}^{K} \left[\mathbf{1}(m(t) = j) \times \mathbf{1}(c(p) = k) \times \mathbf{X}_{pt} \boldsymbol{\beta}_{jk} \right] + \alpha P_{ISO(p),t} + \theta_{p,m(t)} + \gamma_{ISO(p),t} + \varepsilon_{pt} \tag{4}$$

where W_{pt}^{TP} represents average daily water withdrawals for power plant p in time t (year-month). This specification includes an additional indicator function for cooling type, $\mathbf{1}(c(p) = k)$, that allows the impacts of climate to vary both across seasons and cooling technologies (once-through, recirculating, or complex). The term $\theta_{p,m(t)}$ represents a plant-month fixed effect, capturing unobserved heterogeneity specific to each power plant, and $\gamma_{ISO(p),t}$ is an ISO-by-year fixed effect. Lastly, we cluster standard errors at the plant level and by ISO-by-year. We also estimated a simplified version of Equation 4 that excludes the cooling technology indicator function to visualize average effects of climate across the whole study sample. A map of CONUS with plant locations, ISO regions, and transmission constraint boundaries is available in Figure A12. The concentration of power plants in the eastern US reflects the actual distribution of thermoelectric generation infrastructure across CONUS. Fit statistics and more regression information for all sector-specific statistical models are available in Table A3.

[1] The 250 km maximum radius was chosen to ensure that large metropolitan areas were within range of the largest power plants in our sample. We tested different maximum radii from 100 to 500 km, however there were no qualitative changes in results. We can provide these results upon request.

4.2.4 Trends in climate sensitivity

To further investigate the role of adaptation in moderating water use, we explore whether the sensitivity of water withdrawals to climate variables has changed over time. Adaptation to climate change and population growth can manifest in two ways: (1) reducing or increasing overall water use (as captured by time trends) and (2) dampening the marginal effects of climatic factors. For example, improvements in irrigation efficiency may lower total water withdrawals while simultaneously reducing the responsiveness of withdrawals to temperature changes. To test this, we estimate additional model specifications for each sector that allow the coefficients of climate variables to vary by half-decade. For PU, the econometric model takes the form:

$$WPC_{it}^{\text{PU}} = \sum_{j=1}^{12} \sum_{d=1}^{4} \left[\mathbf{1}(m(t) = j) \times \mathbf{1}(D(t) = d) \times \mathbf{X}_{it} \boldsymbol{\beta}_{jd} \right] + \theta_{i,m(t)} + \gamma_{s(i),t} + h_i(t) + \varepsilon_{it}, \qquad (5)$$

where $\mathbf{1}(D(t) = d)$ is an additional indicator function that equals 1 when t falls within half-decade d (e.g., 2000–2004, 2005–2009, etc.), and 0 otherwise. The matrix $\mathbf{X}_{it}$ contains climate and hydrology variables, which interact with both indicator functions to allow the coefficients $\boldsymbol{\beta}_{jd}$ to vary across months and half-decades. If adaptation efforts are effectively reducing climate sensitivity, we would expect coefficients for earlier periods (e.g., 2000–2004) to be larger in magnitude than those for later periods (e.g., 2015–2019). This pattern would suggest that over time, water users have become less responsive to climatic changes, consistent with the adoption of technological improvements, efficiency gains, or behavioral changes. Conversely, stable or increasing coefficients would indicate persistent or even heightened sensitivity to climate, implying either insufficient adaptation or overriding factors such as intensifying climate variability. For CI and TP, water withdrawals are normalized with a log-transformation.

4.2.5 Endogeneity concerns

While our econometric approach provides a robust framework for analyzing sector-specific water use, it is important to address potential endogeneity concerns that may arise from interdependencies in water withdrawals across sectors. These concerns primarily stem from the possibility that water use in one sector could influence usage in others, particularly in regions with constrained water resources.

In the eastern US, where water is generally abundant, an assumption of independence between sectors is reasonable. Water withdrawals for PU, CI, and TP are unlikely to compete directly for resources, as the total water supply exceeds demand across all sectors. In this context, water use within each sector is determined by time-varying, county-specific correlates such as climate and population, as well as fixed effects and time trends. While temporary or localized factors, such as

droughts or water quality issues, could create short-term interdependencies, these are unlikely to meaningfully bias results given the spatial and temporal resolution of our dataset. We acknowledge that such nuances are an inherent limitation of aggregated analyses but argue that they are unlikely to significantly affect our findings.

In the western US, water allocation is governed by the prior appropriation doctrine, which establishes fixed annual allocations for each sector based on historical rights. This system largely separates water use across sectors, as allocations are determined prior to actual withdrawals each year. Changes in the total composition of water rights, including buying and selling, are gradual and captured by the state-year fixed effects in our models. However, it is important to recognize that while this governance structure limits direct interdependencies, multiple factors could introduce endogeneity. First, in many western basins, total water rights allocations exceed actual water availability, particularly during droughts. In these instances, realized withdrawals may reflect cross-sector competition for limited flows rather than allocated rights. Second, short-term leasing of water, particularly in agricultural regions, could create interdependencies as water is reallocated between sectors based on economic or climatic conditions. For example, water rights might be leased from CI to PU during droughts, influencing the observed composition of withdrawals.

To address these concerns, we conducted a robustness check using a Seemingly Unrelated Regression (SUR) approach for PU and CI, as these sectors share a common spatial and temporal structure. This method accounts for potential correlations in residuals across sector-specific models, explicitly allowing for contemporaneous interdependencies in water withdrawals between PU and CI. While TP data was excluded from the SUR due to its plant-level resolution and shorter time span (2008–2020 vs. 2000–2020), the results for PU and CI provide valuable insights. Specifically, if coefficients on key regressors (e.g., temperature and soil moisture) remain stable in magnitude and significance under the SUR framework, it suggests that any interdependencies between these sectors do not meaningfully bias our results. These analyses are available in Section A.1.1 and Figure A13.

We also acknowledge that our approach does not explicitly capture dynamic feedback mechanisms or indirect linkages between sectors. For example, water withdrawals for TP could influence energy prices, which in turn might affect irrigation costs and practices. Similarly, policy interventions prioritizing one sector during droughts could introduce interdependencies that are not fully accounted for by our historical fixed effects. While these factors are important, we argue that their impact on long-term water use patterns is likely small relative to the broader drivers analyzed in this study, such as climate, population growth, and adaptation trends.

4.3 Out-of-sample validation and forecasting performance

To assess the predictive performance of our econometric models, we conducted a series of out-of-sample (OOS) validation exercises. These exercises were implemented separately for each sector and evaluate whether relationships estimated using the historical panel are capable of reproducing observed water use patterns in withheld time periods.

We implemented two complementary validation strategies. First, we conducted a *forecast split*, in which models were estimated using early-period data and evaluated on later observations. For PU and CI, models were trained on data from 2000–2009 and used to predict water withdrawals for 2010–2019. For TP, which has a shorter time series, models were trained on 2008–2013 and evaluated on 2014–2019. Second, we implemented a *temporally structured cross-validation* procedure using five contiguous folds of years. In each fold, models were trained on four subsets of years and evaluated on the held-out block, ensuring that training and testing data were separated in time.

In both exercises, model performance was evaluated by comparing observed and predicted values of water withdrawals at the monthly county (PU, CI) or plant (TP) level. Figure A14 presents these results, displaying observed versus predicted values along with the corresponding OOS R^2 statistics. Across all sectors, the models exhibit strong predictive performance, with OOS R^2 values ranging from 0.87 to 0.98 depending on the sector and validation approach.

It is important to interpret these results in the context of the modeling framework. These validation exercises were conducted using specifications that retain persistent fixed effects (e.g., county-month or plant-month effects) but exclude time-specific fixed effects (e.g., state-year or ISO-year effects), which are not forecastable outside the estimation sample. As a result, the models leverage stable, location-specific seasonal patterns in water use, along with estimated responses to climate, hydrology, and population, to generate predictions in held-out years.

More fundamentally, these models are designed to estimate marginal responses to hydroclimatic and socioeconomic drivers, rather than to independently forecast long-run levels of water use. This structure has two implications for interpreting out-of-sample fit. First, because persistent spatial and seasonal components of water use are well captured by fixed effects, the models are able to reproduce observed levels with high accuracy in held-out periods. Second, because projections are anchored to historical averages and expressed as deviations from those baselines, the high predictive fit observed in Figure A14 reflects the model's ability to recover stable patterns and marginal responses, rather than its ability to generate fully independent forecasts of future water use.

4.4 Estimating future water demands

To project changes in future water use, we applied the estimated sector-specific coefficients ($\hat{\boldsymbol{\beta}}$, $\hat{\alpha}$) and time trends ($\hat{h}_i$) from equations 1, 2, and 4 to the projected data for each of the 28 future

scenarios. We calculated changes in the averages of the climate and hydrology variables ($\bar{\mathbf{X}}$) for each county (i) or power plant (p) under each future scenario (f), relative to the observed 2000–2020 period (obs), as $\Delta\mathbf{X}^f = \bar{\mathbf{X}}^f - \bar{\mathbf{X}}^{obs}$. Similarly, we calculated changes in county and ISO populations as $\Delta P^f = \bar{P}^f - \bar{P}^{obs}$. The changes in water use for each sector were thus calculated as:

$$\Delta WPC_i^{\mathrm{PU},f} = \sum_{j=1}^{12} \left[\mathbf{1}(m(t)=j) \times \Delta\mathbf{X}_i^f \hat{\boldsymbol{\beta}}_j\right] + \Delta\hat{h}_i, \tag{6}$$

$$\Delta W_i^{\mathrm{CI},f} = \sum_{j=1}^{12}\sum_{r=1}^{R} \left[\mathbf{1}(m(t)=j) \times \mathbf{1}(FRR(i)=r) \times \Delta\mathbf{X}_i^f \hat{\boldsymbol{\beta}}_{jr}\right] + \hat{\alpha}\Delta P_i^f + \Delta\hat{h}_i, \tag{7}$$

$$\Delta W_p^{\mathrm{TP},f} = \sum_{j=1}^{12}\sum_{k=1}^{K} \left[\mathbf{1}(m(t)=j) \times \mathbf{1}(c(p)=k) \times \Delta\mathbf{X}_p^f \hat{\boldsymbol{\beta}}_{jk}\right] + \hat{\alpha}\Delta P_{ISO(p)}^f, \tag{8}$$

where $\Delta\hat{h}_i = \hat{h}_i(2055) - \hat{h}_i(2020)$, representing the difference between the midpoint of the future period and the end of the baseline period, respectively. Here, projected changes in water use implicitly incorporate adaptation through the continuation of estimated county-specific time trends, which addresses a key limitation of projection methods that abstract from long-run behavioral adjustment [72, 76–78].

Because the statistical specifications include high-dimensional fixed effects, the models identify marginal responses to changes in climate, hydrology, and population rather than absolute levels of water use. These fixed effects absorb persistent baseline differences across locations and are not forecastable outside the estimation sample. Accordingly, projections are constructed as changes relative to observed historical conditions. Future levels are then recovered by adding these projected changes to observed average baselines:

$$\bar{WPC}_i^{\mathrm{PU},f} = \bar{WPC}_i^{\mathrm{PU},obs} + \Delta WPC_i^{\mathrm{PU},f}, \tag{9}$$

$$\bar{W}_i^{\mathrm{CI},f} = \bar{W}_i^{\mathrm{CI},obs} + \Delta W_i^{\mathrm{CI},f}, \tag{10}$$

$$\bar{W}_p^{\mathrm{TP},f} = \bar{W}_p^{\mathrm{TP},obs} + \Delta W_p^{\mathrm{TP},f}, \tag{11}$$

where $\bar{WPC}_i^{\mathrm{PU},obs}$, $\bar{W}_i^{\mathrm{CI},obs}$, and $\bar{W}_p^{\mathrm{TP},obs}$ represent the observed average water withdrawals per capita for PU, CI water withdrawals, and TP water withdrawals during the 2000–2020 period, respectively. $\bar{WPC}_i^{\mathrm{PU},f}$ was then multiplied by the projected population for county i under scenario f to estimate total withdrawals for public use: $\bar{W}_i^{\mathrm{PU},f}$.

Lastly, adjustments were made to $\bar{W}_p^{\mathrm{TP},f}$ to incorporate state-level clean energy goals into the projections for thermoelectric power generation. There are currently 24 states that have committed to achieving 100% clean energy by 2030-2050 [46], which implies the gradual phase-out of coal and

natural gas power plants. For coal and gas plants located in states with such goals, future TP water withdrawals were set to zero ($\bar{W}_p^{\mathrm{TP},f} = 0$) by the state's target date. This adjustment reflects the anticipated shift towards renewable energy sources, which generally require less water for cooling. The states and their clean energy goals are summarized in Table A4, and the phase-out of withdrawals is applied proportionally over time to capture the gradual nature of the transition. Additionally, all plants with zero withdrawals over 2018-2020 were assumed retired and therefore also had future withdrawals set to zero. These adjustments ensured that the projected water use for thermoelectric power generation reflected both observed relationships in the historical data and expected structural changes in the energy sector, providing a more realistic estimate of future TP water demands.

4.4.1 Disentangling future drivers

To illustrate the relative contributions of climate and hydrology, population growth, and the continuation of historical trends to future water use, we decomposed projected changes from Equations 6–8 into separate components. For each sector and scenario, we first isolated the effect of climate and hydrology by holding population and demand trends constant at their baseline values and substituting only the projected changes in monthly climate and hydrology variables: $\sum_{j=1}^{12} \left[\mathbf{1}(m(t) = j) \times (\bar{\mathbf{X}}_i^f - \bar{\mathbf{X}}_i^{obs})\,\hat{\boldsymbol{\beta}}_j\right]$ or the analogous expressions for crop irrigation and thermoelectric generation. This term captures the change in withdrawals attributable solely to deviations in future climate and hydrology relative to 2000–2020 means. Similarly, the effect of population was then calculated from: $\hat{\alpha}\,(\bar{P}_i^f - \bar{P}_i^{obs})$, or, for public supply, by multiplying the projected change in per capita withdrawals by the projected change in population for each county. Lastly, the contribution of other trends was taken as the change in the fitted county-specific time trends between the midpoint of the projection period and the end of the baseline period: $\Delta\hat{h}_i = \hat{h}_i(2055) - \hat{h}_i(2020)$, representing the net effect of observed adaptation or other unmeasured drivers.

4.5 Characterizing future water scarcity

To assess future water scarcity within the US, we calculated a withdrawal-to-availability (WTA) ratio for the observed historical period and under all future scenarios. The WTA ratio measures relative water scarcity as the ratio of total annual withdrawals to annual *renewable* water resources [79, 80]. Here, total water withdrawals were calculated as the sum of all estimated withdrawals for PU, CI, and TP for each county:

$$T\bar{W}_i^f = \bar{W}_i^{\mathrm{PU},f} + \bar{W}_i^{\mathrm{CI},f} + \bar{W}_i^{\mathrm{TP},f}, \tag{12}$$

where $\bar{W}$ is the average annual withdrawals across all future periods under scenario f and $\bar{W}_i^{\mathrm{TP},f}$ is the sum of withdrawals across all power plants within county i's boundaries.

While WTA ratios can be calculated at the county level, they may not fully capture water scarcity dynamics in the US, given the extensive network of dams, reservoirs, and inter-basin transfers that deliver water across county boundaries. These systems redistribute water from areas of surplus to areas with higher demand, reducing the significance of highly localized WTA values. To account for this, we aggregated total withdrawals across counties to larger watersheds. Specifically, we aggregated to the HUC04 hydrologic unit code as classified by the USGS, which divides the conterminous US into 208 subregions, compared to the 3,108 counties. This spatial aggregation provided a more meaningful assessment of water availability and stress across regions that share hydrologic and water management systems.

For total renewable water availability, we used the total amount of runoff (R) within a watershed, as estimated by the VIC model. Total runoff comprises both surface and subsurface runoff, and represents the volume of water that flows into lakes and rivers, a portion of which could be feasibly stored in reservoirs. The WTA ratio was thus calculated as:

$$WTA_h^f = \frac{T\bar{W}_h^f}{R_h^f}, \tag{13}$$

for hydrologic unit code h under scenario f. As WTA increases, reliance on nonlocal and nonrenewable water sources grows. Following Hanasaki et al. [81], water stress thresholds were defined as follows (where "water scarcity" refers to general water insufficiency and "water stress" describes when WTA exceeds certain thresholds):

1. **Low water stress (WTA $<$ 0.2)**: Indicates relatively sustainable water use. At this level, the required water can be supplied almost entirely by local, renewable water resources.
2. **Moderate water stress (WTA 0.2 to 0.4)**: Local renewable water is not sufficient to meet all demands, and reliance on nonlocal or nonrenewable water sources begins (e.g., groundwater).
3. **High water stress (WTA 0.4 to 1.0):** A significant portion of water demand must be met by nonlocal or nonrenewable sources.
4. **Very high water stress (WTA 1 to 2):** Local renewable resources are insufficient, and reliance on external sources becomes necessary.
5. **Severe water stress (WTA 2 to 10):** Critical dependence on nonrenewable groundwater or water imports.
6. **Extreme water stress (WTA $>$ 10):** Nearly all water demand must be supplied by nonlocal or nonrenewable water sources.

These thresholds provide a simple framework for evaluating water stress across future scenarios. For regions where WTA remains below 0.2, water use can generally be considered sustainable, with

sufficient renewable water to meet local demand. A region is considered water-scarce when WTA exceeds 0.2 and severely water-scarce beyond 0.4 [80].

4.6 Counterfactual policy analysis

While the baseline projections incorporate both projected changes in climate and population, as well as the continuation of historical adaptation and energy sector transitions, these assumptions may not hold under alternative technological or policy pathways. To evaluate the role of these factors in shaping future water demand, we construct a set of counterfactual scenarios that isolate the effects of adaptation and efficiency improvements.

All counterfactual scenarios are evaluated relative to the "Moderate" (SSP245) scenario, which serves as the baseline case. This scenario reflects intermediate warming, population growth, and hydrologic change, and includes both the continuation of county-specific time trends and the implementation of state-level clean energy goals in the thermoelectric sector. From this baseline, we consider four alternative scenarios:

1. *Improved irrigation efficiency:* Modeled increases in irrigation withdrawals were reduced by 20%, reflecting the adoption of more efficient irrigation technologies or practices (e.g., sprinkler, drip, or deficit irrigation). Negative changes in irrigation demand were left unchanged.
2. *Improved thermoelectric efficiency:* All power plants were assumed to operate using recirculating cooling systems. This was implemented by applying the estimated coefficients for recirculating technologies to all plants when predicting future water withdrawals, while retaining baseline assumptions about plant retirements.
3. *Combined efficiency:* This scenario incorporated both improved irrigation efficiency and improved thermoelectric cooling efficiency.
4. *No adaptation:* Projected time trends are removed from Equations 6 and 7 by setting $\Delta\hat{h}_i = 0$, thereby holding adaptation-related changes in water use fixed at their baseline levels. In addition, energy sector transitions are removed by relaxing the retirement assumptions applied to thermoelectric power plants, allowing all plants to continue operating under their historical characteristics.

By comparing outcomes across these scenarios relative to the baseline case, we can isolate the contributions of continued adaptation, as well as the efficacy of different policy approaches to reduce water demands.

4.7 Limitations

The methods used in this study are subject to several limitations that should be acknowledged when interpreting the results. We assume that the relationship between hydro-climate and population variables and water withdrawals can be adequately captured by a model that is linear in parameters. While linear models provide an efficient and unbiased estimation of average effects, it may oversimplify real-world dynamics, particularly in cases where threshold effects or nonlinear relationships are present. Additionally, there is some debate as to whether the econometric methods employed in this study fully account for adaptation by economic agents. Some scholars have noted that models like the ones used here could overestimate future impacts by failing to incorporate behavioral or technological adaptations to climate change [77]. Estimating the net impacts of such adaptive measures remains a challenge, but it is critical for a complete understanding of the economic implications of climate change [72]. Regardless, our use of time trends and incorporating state-level energy plans should account for some adaptive behavior. We also test for changing climate sensitivity (e.g., marginal effects of temperature) over time.

For thermoelectric power generation, the assumption that coal and gas plants in states with 100% clean energy goals will cease operations by 2050 may oversimplify the energy market. Plants could remain in operation within a state with a clean energy portfolio if they sell electricity to utilities in neighboring states without clean energy mandates. Additionally, due to data limitations, we only consider water withdrawals for thermoelectric power, and therefore do not estimate the withdrawals necessary to support the renewable energy sources that may replace the retired coal and natural gas plants.

There are also several critiques of using the WTA ratio to characterize water scarcity. First, runoff may not fully capture the amount of water that can be made available for human use, and withdrawals do not account for consumptive use [82]. However, WTA has been shown to be globally robust, with the 20% threshold representing conditions where daily water requirements cannot be consistently met without reservoirs, aqueducts, or other infrastructure [81]. Secondly, WTA does not consider green water (soil moisture) or water quality, both of which may exacerbate scarcity [83]. In this study, projected withdrawals are influenced by soil moisture, which partially captures its effect. Lastly, WTA thresholds are often defined assuming a 30% environmental flow requirement [84], which may vary across geographies.

In addition to these hydrologic considerations, it is important to acknowledge that the WTA ratio does not reflect traditional economic definitions of scarcity, which emphasize the role of prices in equilibrating supply and demand. From an economic perspective, scarcity arises when the quantity demanded exceeds the quantity supplied at the prevailing price, and in well-functioning markets, this

imbalance should be resolved through price adjustments or reallocation. In contrast, the WTA ratio is a physical measure that compares total water withdrawals to renewable supply, without accounting for institutional constraints, allocation mechanisms, or price signals. High WTA values may reflect biophysical limitations, rising demand, or rigidities in allocation systems—not necessarily inefficient use. Nevertheless, in the US context where water allocation is often determined administratively and prices do not fully reflect scarcity, the WTA ratio offers a useful proxy for assessing potential stress on renewable water resources. Our projected withdrawals incorporate both demand-side factors, such as population growth and observed reductions in water use over time, and climate-driven variation in supply, providing a plausible assessment of future pressures. While the WTA metric itself does not reflect market-based scarcity or reallocation, our modeling approach captures behavioral and institutional responses indirectly through estimated time trends and climatic responses.

5 Disclaimer and Acknowledgment

The findings and conclusions in this report are those of the authors and should not be construed to represent any official USDA or US Government determination or policy. This research was supported [in part] by the US Department of Agriculture, Forest Service.

6 Figures

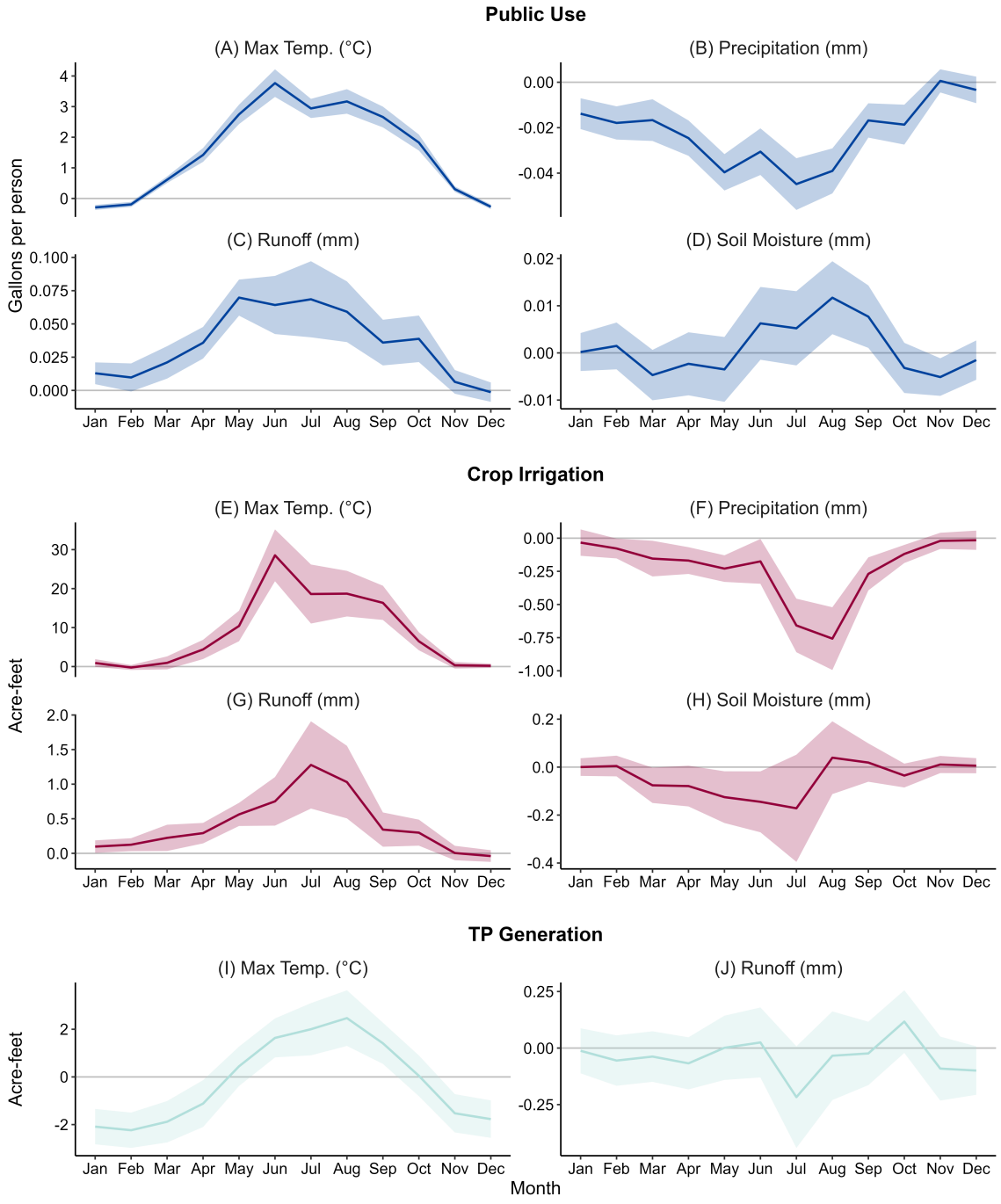


Fig. 1 Estimated seasonal marginal effects of the impacts of climate and hydrology on water withdrawals for public use, crop irrigation, and cooling for thermoelectric power generation. Confidence intervals are at the 95% level. For visual purposes, marginal effects for crop irrigation and thermoelectric power cooling correspond to the specifications of Equation 2 and Equation 4 that exclude the indicator functions for region and cooling technology, respectively, and each plot has a unique scale to showcase seasonality. Precipitation and soil moisture are not included in the model for TP generation.

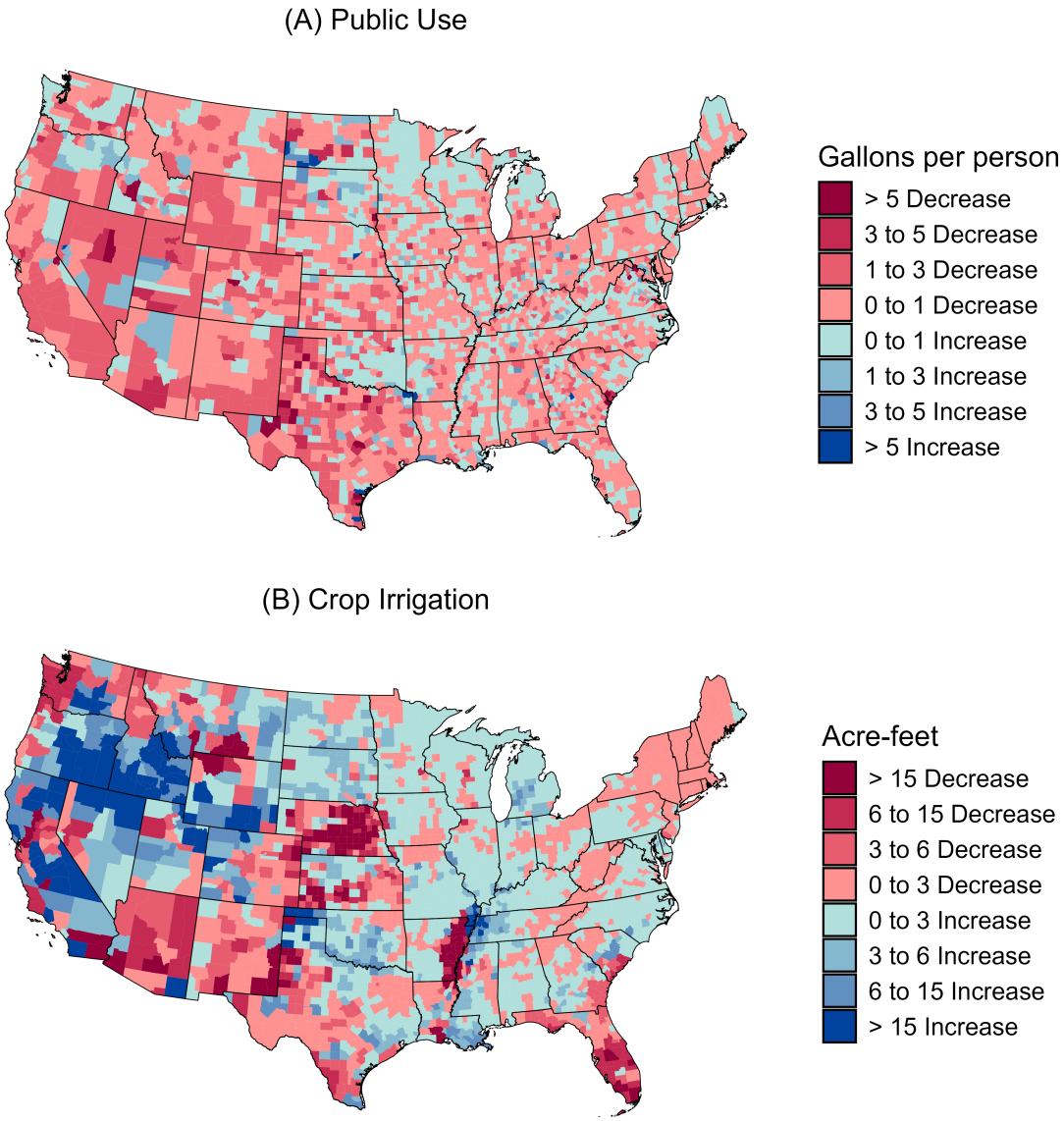


Fig. 2 Annual water use trends for public use (gallons per person per day) and crop irrigation (acre-feet per day) after controlling for climate, hydrology, population, and unobserved confounding variables over the historical (2000-2020) period. Coloring corresponds to the slope of the county-specific linear time trend ($h_i(t)$) from Equation 1 (public use) and Equation 2 (crop irrigation), where blue (red) indicates increasing (decreasing) water use. Statistically significant trends are reported in Figure A6.

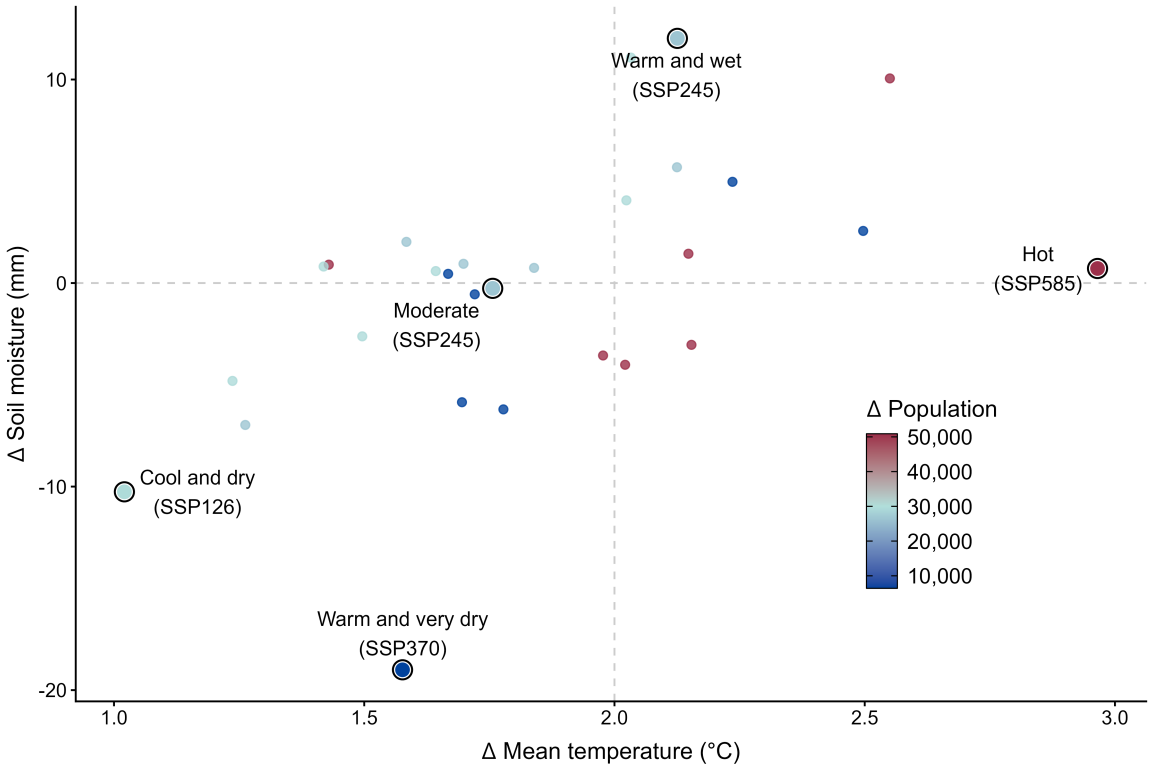


Fig. 3 Stylized climate and population scenarios selected from the full ensemble of CMIP6 projections. Each point represents a GCM paired with an SSP, plotted in temperature–soil moisture space using projected changes over 2040–2070 relative to 2000–2020. Point color indicates projected average, county-level population change. Highlighted points denote the five scenarios used for analysis: *Cool and dry* (low warming, large moisture deficit; GCM: MPI-ESM1-2-HR), *Warm and very dry* (moderate warming with severe drying; GCM: MPI-ESM1-2-HR), *Moderate* (intermediate conditions; GCM: BCC-CSM2-MR), *Warm and wet* (moderate warming with increased moisture; GCM: ACCESS-CM2), and *Hot* (high warming with modest moisture change; GCM: EC-Earth3). These scenarios span the joint distribution of temperature, hydrologic change, and population growth.

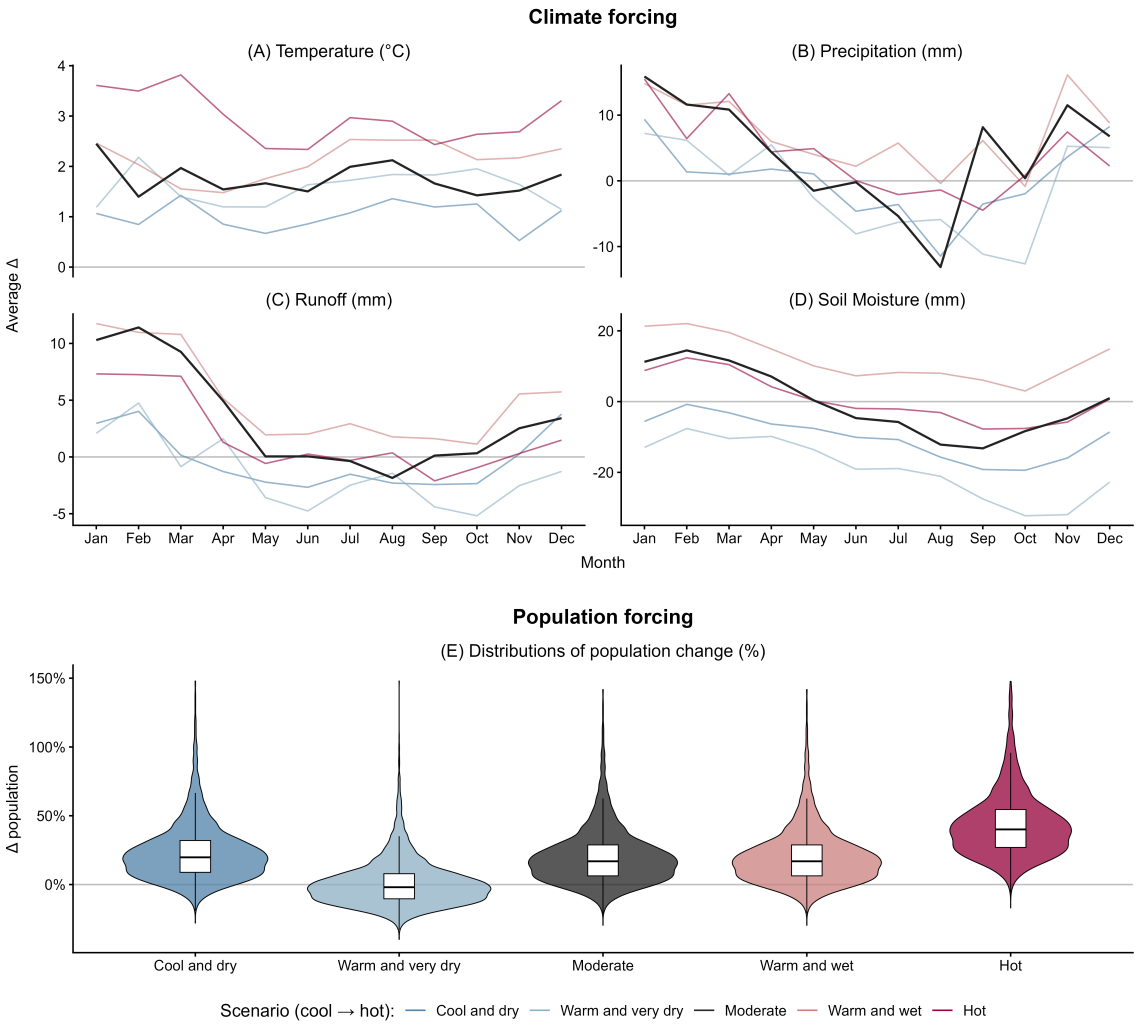


Fig. 4 Projected changes in climate and population across stylized future scenarios (2040–2070 relative to 2000–2020). Panels (A)–(D) show monthly average changes in a subset of hydroclimatic variables: temperature, precipitation, runoff, and soil moisture. Lines correspond to scenario-specific averages across counties, with the *Moderate* scenario in black for reference. Panel (E) shows the distribution of projected population change across counties for each scenario. Population growth varies substantially across scenarios, ranging from near-zero or negative growth in low-growth scenarios to substantial increases in high-growth scenarios, reflecting differences in SSP assumptions.

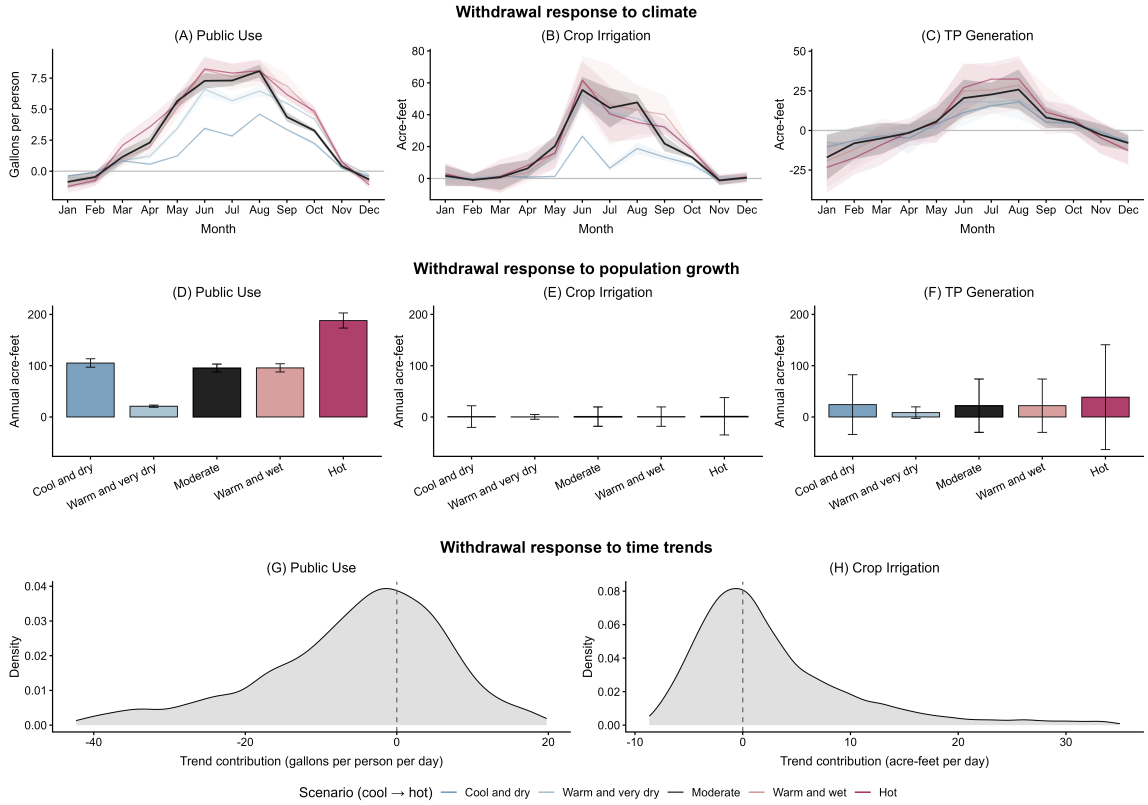


Fig. 5 Estimated changes in water withdrawals driven by climate, population growth, and long-run trends across sectors. Panels (A)–(C) show average monthly withdrawal responses attributable to climate change for public use (PU), crop irrigation (CI), and thermoelectric power (TP), respectively. Shaded regions denote 95% confidence intervals. Panels (D)–(F) display annual changes in withdrawals attributable to population growth. Error bars reflect uncertainty in estimated population effects. Panels (G)–(H) show the distribution of county-level time trends, which capture the net effect of technological change, policy, and behavioral adaptation not explained by observed variables. No time trends were estimated for TP due to the shorter sample period.

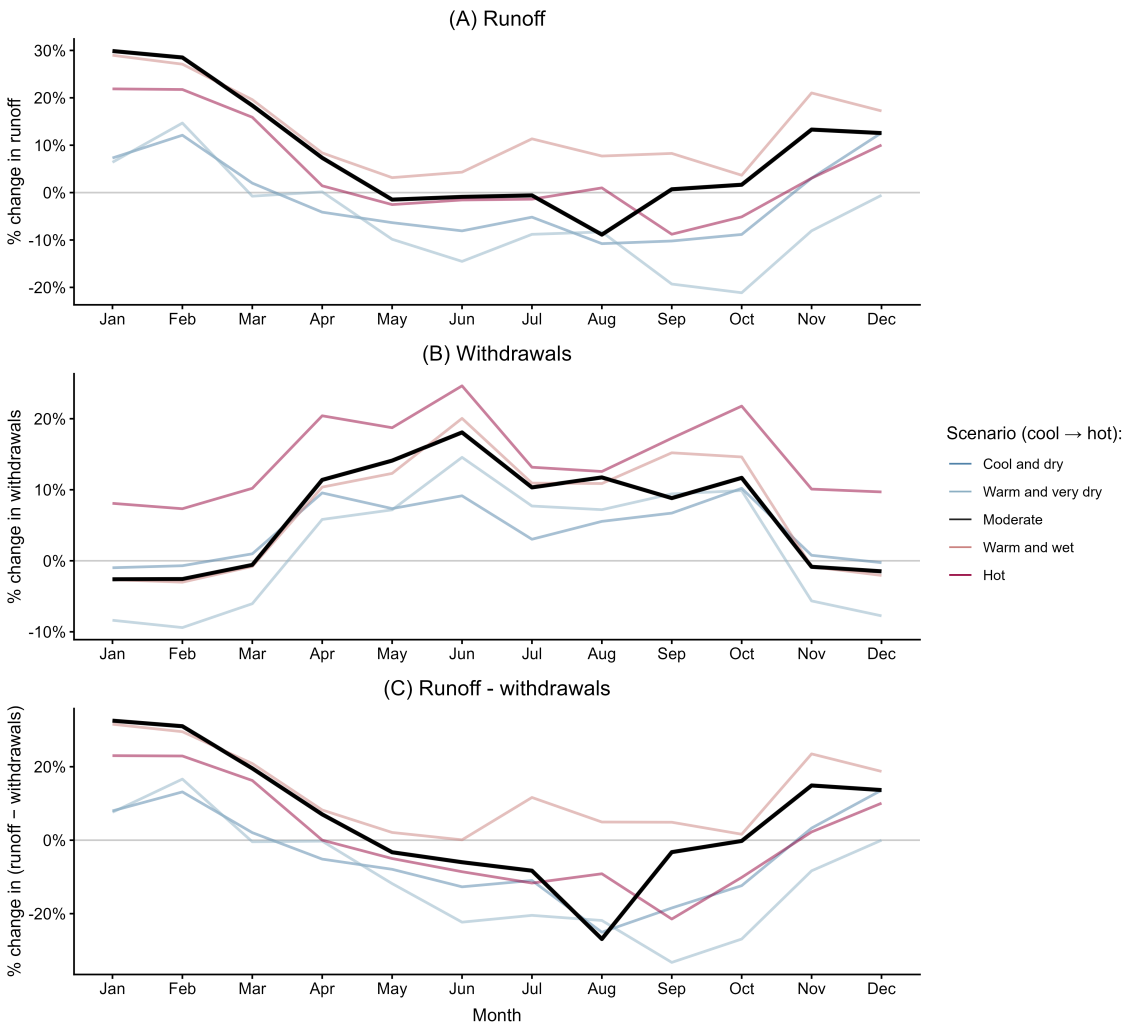


Fig. 6 Projected total monthly changes (2040–2070) in (A) runoff, (B) water withdrawals, and (C) the net difference between water availability and withdrawals, relative to the observed baseline period (2000–2020), for CONUS. Panel (A) captures changes in water supply driven by hydroclimatic conditions, while panel (B) reflects changes in water demand. Panel (C) combines these effects to show net changes in water scarcity. Positive values in panel (C) indicate an increase in excess supply (improved water availability relative to demand), while negative values indicate a reduction in excess supply (worsening water scarcity). The moderate scenario is highlighted in black.

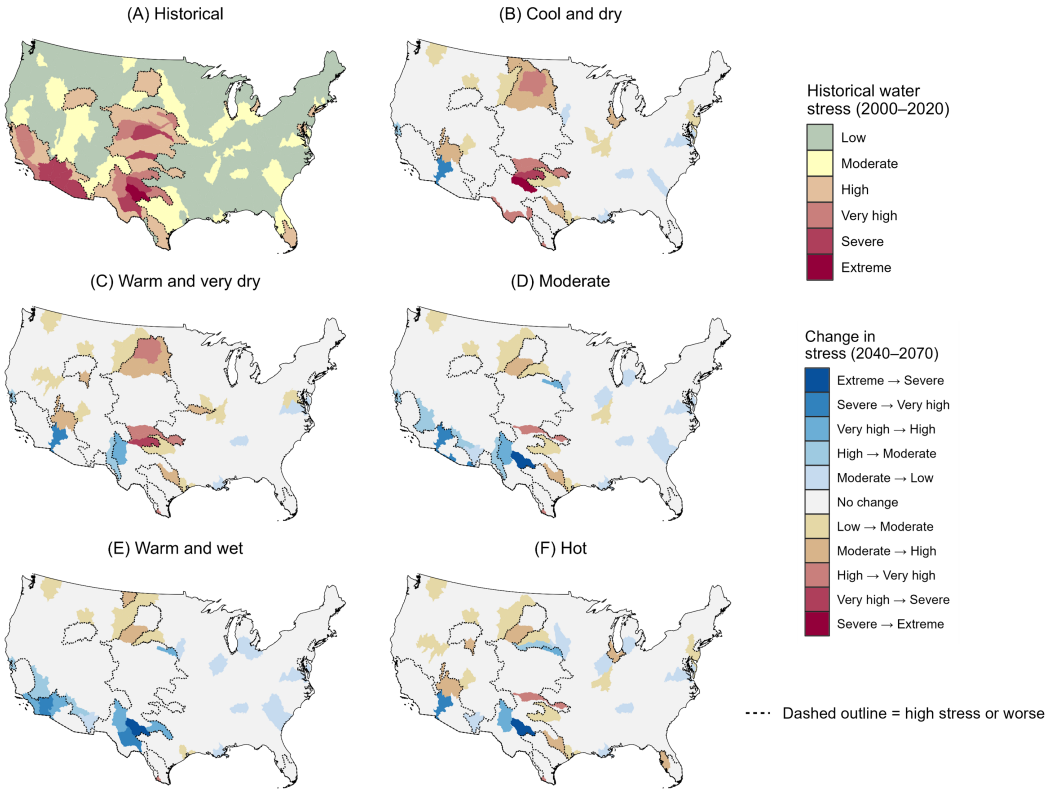


Fig. 7 Projected changes in water scarcity across five climate-population scenarios (2040–2070) relative to the historical baseline (2000–2020), shown by HUC04 subregion. Panel (A) displays historical water stress categories, while panels (B–F) show transitions in water stress under each future scenario. Colors represent transitions in water stress categories, with blue indicating improvements (movement to lower stress categories), red indicating worsening conditions, and light gray indicating no change. Dashed outlines indicate regions experiencing high water stress or worse (WTA ≥ 0.4).

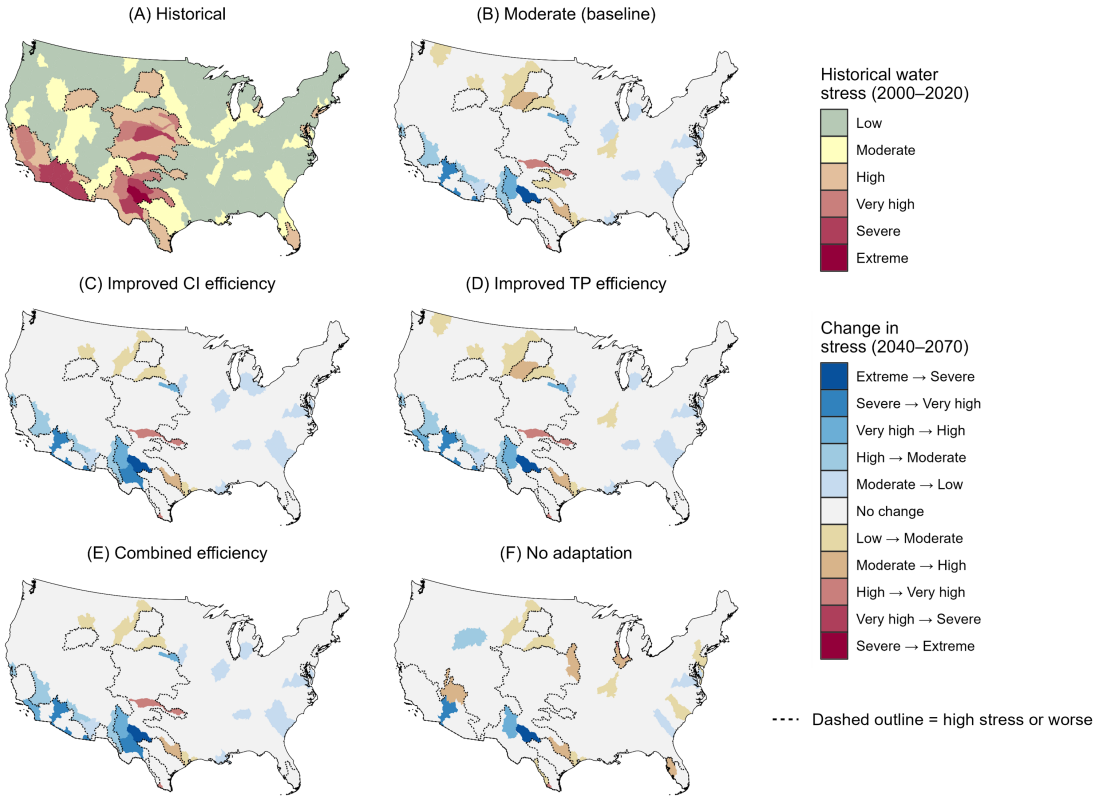


Fig. 8 Projected changes in water scarcity across counterfactual scenarios (2040–2070) relative to the historical baseline (2000–2020), shown by HUC04 subregion. Panel (A) displays historical water stress categories, while panel (B) shows changes under the "Moderate" (baseline) scenario. Panels (C)–(F) present changes under alternative scenarios. Colors represent transitions in water stress categories, with blue indicating improvements (movement to lower stress categories), red indicating worsening conditions, and light gray indicating no change. Dashed outlines indicate regions experiencing high water stress or worse (WTA ≥ 0.4).

References

[1] Gosling, S.N., Arnell, N.W.: A global assessment of the impact of climate change on water scarcity. Climatic Change **134**, 371–385 (2016)

[2] Mekonnen, M.M., Hoekstra, A.Y.: Four billion people facing severe water scarcity. Science advances **2**(2), 1500323 (2016)

[3] He, C., Liu, Z., Wu, J., Pan, X., Fang, Z., Li, J., Bryan, B.A.: Future global urban water scarcity and potential solutions. Nature Communications **12**(1), 4667 (2021)

[4] Marston, L., Konar, M., Cai, X., Troy, T.J.: Virtual groundwater transfers from overexploited aquifers in the united states. Proceedings of the National Academy of Sciences **112**(28), 8561–8566 (2015)

[5] Lindqvist, A.N., Fornell, R., Prade, T., Tufvesson, L., Khalil, S., Kopainsky, B.: Human-water dynamics and their role for seasonal water scarcity–a case study. Water Resources Management **35**, 3043–3061 (2021)

[6] Caretta, M.A., Mukherji, A., Arfanuzzaman, M., Betts, R.A., Gelfan, A., Hirabayashi, Y., Lissner, T.K., Liu, J., Lopez Gunn, E., Morgan, R., Mwanga, S., Supratid, S.: Water. In: Pörtner, H.-O., Roberts, D.C., Tignor, M., Poloczanska, E.S., Mintenbeck, K., Alegría, A., Craig, M., Langsdorf, S., Löschke, S., Möller, V., Okem, A., Rama, B. (eds.) Climate Change 2022: Impacts, Adaptation and Vulnerability. Contribution of Working Group II to the Sixth Assessment Report of the Intergovernmental Panel on Climate Change, pp. 551–712. Cambridge University Press, Cambridge, UK and New York, NY, USA (2022). https://doi.org/10.1017/9781009325844.006

[7] Earman, S., Dettinger, M.: Potential impacts of climate change on groundwater resources–a global review. Journal of water and climate change **2**(4), 213–229 (2011)

[8] Douville, H., Raghavan, K., Renwick, J., Allan, R.P., Arias, P.A., Barlow, M., Cerezo-Mota, R., Cherchi, A., Gan, T.Y., Gergis, J., Jiang, D., Khan, A., Pokam Mba, W., Rosenfeld, D., Tierney, J., Zolina, O.: Water cycle changes. In: Masson-Delmotte, V., Zhai, P., Pirani, A., Connors, S.L., Péan, C., Berger, S., Caud, N., Chen, Y., Goldfarb, L., Gomis, M.I., Huang, M., Leitzell, K., Lonnoy, E., Matthews, J.B.R., Maycock, T.K., Waterfield, T., Yelekçi, O., Yu, R., Zhou, B. (eds.) Climate Change 2021: The Physical Science Basis. Contribution of Working Group I to the Sixth Assessment Report of the Intergovernmental Panel on Climate Change, pp. 1055–1210. Cambridge University Press, Cambridge, United Kingdom and New York, NY, USA (2021). https://doi.org/10.1017/9781009157896.010

[9] Gordon, B.L., Brooks, P.D., Krogh, S.A., Boisrame, G.F., Carroll, R.W., McNamara, J.P., Harpold, A.A.: Why does snowmelt-driven streamflow response to warming vary? a data-driven review and predictive framework. Environmental Research Letters **17**(5), 053004 (2022)

[10] Richter, B.D., Ao, Y., Lamsal, G., Wei, D., Amaya, M., Marston, L., Davis, K.F.: Alleviating water scarcity by optimizing crop mixes. Nature Water **1**(12), 1035–1047 (2023)

[11] Dolan, F., Lamontagne, J., Link, R., Hejazi, M., Reed, P., Edmonds, J.: Evaluating the economic impact of water scarcity in a changing world. Nature communications **12**(1), 1–10 (2021)

[12] Barbier, E.B., Burgess, J.C.: Economics of water scarcity and efficiency. Sustainability **16**(19), 8550 (2024)

[13] Zografos, C., Goulden, M.C., Kallis, G.: Sources of human insecurity in the face of hydro-climatic change. Global environmental change **29**, 327–336 (2014)

[14] Dinar, S., Katz, D., De Stefano, L., Blankespoor, B.: Climate change, conflict, and cooperation: Global analysis of the effectiveness of international river treaties in addressing water variability. Political geography **45**, 55–66 (2015)

[15] Unfried, K., Kis-Katos, K., Poser, T.: Water scarcity and social conflict. Journal of Environmental Economics and Management **113**, 102633 (2022)

[16] Khan, S.J., Deere, D., Leusch, F.D., Humpage, A., Jenkins, M., Cunliffe, D.: Extreme weather events: Should drinking water quality management systems adapt to changing risk profiles? Water research **85**, 124–136 (2015)

[17] Scheffers, B.R., De Meester, L., Bridge, T.C., Hoffmann, A.A., Pandolfi, J.M., Corlett, R.T., Butchart, S.H., Pearce-Kelly, P., Kovacs, K.M., Dudgeon, D., *et al.*: The broad footprint of climate change from genes to biomes to people. Science **354**(6313), 7671 (2016)

[18] Myers, B.J., Lynch, A.J., Bunnell, D.B., Chu, C., Falke, J.A., Kovach, R.P., Krabbenhoft, T.J., Kwak, T.J., Paukert, C.P.: Global synthesis of the documented and projected effects of climate change on inland fishes. Reviews in Fish Biology and Fisheries **27**, 339–361 (2017)

[19] Porter, J.R., Xie, L., Challinor, A.J., Cochrane, K., Howden, S.M., Iqbal, M.M., Lobell, D.B., Travasso, M.I.: Food security and food production systems. In: Field, C.B., Barros, V.R., Dokken, D.J., Mach, K.J., Mastrandrea, M.D., Bilir, T.E., Chatterjee, M., Ebi, K.L., Estrada, Y.O., Genova, R.C., Girma, B., Kissel, E.S., Levy, A.N., MacCracken, S., Mastrandrea, P.R., White, L.L. (eds.) Climate Change 2014: Impacts, Adaptation, and Vulnerability. Part A: Global

781 and Sectoral Aspects. Contribution of Working Group II to the Fifth Assessment Report of
782 the Intergovernmental Panel on Climate Change, pp. 485–533. Cambridge University Press,
783 Cambridge, United Kingdom and New York, NY, USA (2014)

784 [20] Kim, W., Iizumi, T., Nishimori, M.: Global patterns of crop production losses associated with
785 droughts from 1983 to 2009. Journal of Applied Meteorology and Climatology **58**(6), 1233–1244
786 (2019)

787 [21] Leng, G., Hall, J.: Crop yield sensitivity of global major agricultural countries to droughts and
788 the projected changes in the future. Sci. Total. Environ. **654**, 811–821 (2019) https://doi.org/
789 10.1016/j.scitotenv.2018.10.434

790 [22] Rosa, L., *et al.*: Global agricultural economic water scarcity. Sci. Adv. **6**(18), 6031 (2020) https:
791 //doi.org/10.1126/sciadv.aaz6031

792 [23] Qin, Y., Hong, C., Zhao, H., Siebert, S., Abatzoglou, J.T., Huning, L.S., Sloat, L.L., Park, S., Li,
793 S., Munroe, D.K., *et al.*: Snowmelt risk telecouplings for irrigated agriculture. Nature Climate
794 Change **12**(11), 1007–1015 (2022)

795 [24] Van Vliet, M.T., Yearsley, J.R., Ludwig, F., Vögele, S., Lettenmaier, D.P., Kabat, P.: Vulner-
796 ability of us and european electricity supply to climate change. Nature Climate Change **2**(9),
797 676–681 (2012)

798 [25] Yalew, S.G., *et al.*: Impacts of climate change on energy systems in global and regional scenarios.
799 Nat. Energy **5**(10), 794–802 (2020) https://doi.org/10.1038/s41560-020-0664-z

800 [26] Maia-Silva, D., Kumar, R., Nateghi, R.: The critical role of humidity in modeling summer
801 electricity demand across the united states. Nat. Commun. **11**(1), 1686 (2020) https://doi.org/
802 10.1038/s41467-020-15393-8

803 [27] Djehdian, L.A., Chini, C.M., Marston, L., Konar, M., Stillwell, A.S.: Exposure of urban food–
804 energy–water (few) systems to water scarcity. Sustainable Cities and Society **50**, 101621 (2019)

805 [28] Heidari, H., Arabi, M., Warziniack, T.: Vulnerability to water shortage under current and future
806 water supply-demand conditions across us river basins. Earth's Future **9**(10), 2021–002278
807 (2021)

808 [29] Gharib, A.A., Blumberg, J., Manning, D.T., Goemans, C., Arabi, M.: Assessment of vulnera-
809 bility to water shortage in semi-arid river basins: The value of demand reduction and storage
810 capacity. Science of The Total Environment **871**, 161964 (2023)

[30] Colby, B., Hansen, K., Sorensen, K.: Policy nook—policy note: Tough tradeoffs in the colorado river basin. Water Economics and Policy **11**(04), 2471002 (2025)

[31] Dierauer, J.R., Allen, D.M., Whitfield, P.H.: Snow drought risk and susceptibility in the western united states and southwestern canada. Water Resources Research **55**(4), 3076–3091 (2019)

[32] National Integrated Drought Information System (NIDIS): Snow Drought Current Conditions and Impacts in the West. https://www.drought.gov/drought-status-updates/snow-drought-current-conditions-and-impacts-west-2026-02-05 (2026)

[33] Lesinger, K., Tian, D.: Trends, variability, and drivers of flash droughts in the contiguous united states. Water Resources Research **58**(9), 2022–032186 (2022)

[34] Libecap, G.D.: Institutional path dependence in climate adaptation: Coman's "some unsettled problems of irrigation". American Economic Review **101**(1), 64–80 (2011)

[35] Debaere, P., Kurzendoerfer, A.: Decomposing us water withdrawal since 1950. Journal of the Association of Environmental and Resource Economists **4**(1), 155–196 (2017)

[36] Koop, S.H., Van Dorssen, A., Brouwer, S.: Enhancing domestic water conservation behaviour: A review of empirical studies on influencing tactics. Journal of environmental management **247**, 867–876 (2019)

[37] West, J., Fairlie, R.W., Pratt, B., Rose, L.: Automated enforcement of irrigation regulations and social pressure for water conservation. Journal of the Association of Environmental and Resource Economists **8**(6), 1179–1207 (2021)

[38] Blumberg, J., Goemans, C., Manning, D.: Perceived water scarcity and irrigation technology adoption. American Agriculture, Water Resources, and Climate Change, 173 (2024)

[39] Jones, E.R., Bierkens, M.F., Vliet, M.T.: Current and future global water scarcity intensifies when accounting for surface water quality. Nature Climate Change **14**(6), 629–635 (2024)

[40] Rosa, L., Sangiorgio, M.: Global water gaps under future warming levels. Nature Communications **16**(1), 1192 (2025)

[41] Calvin, K., Patel, P., Clarke, L., Asrar, G., Bond-Lamberty, B., Cui, R.Y., Di Vittorio, A., Dorheim, K., Edmonds, J., Hartin, C., Hejazi, M., Horowitz, R., Iyer, G., Kyle, P., Kim, S., Link, R., McJeon, H., Smith, S.J., Snyder, A., Waldhoff, S., Wise, M.: Gcam v5.1: representing the linkages between energy, water, land, climate, and economic systems. Geoscientific Model

Development **12**(2), 677–698 (2019) https://doi.org/10.5194/gmd-12-677-2019

[42] Binsted, M., Iyer, G., Patel, P., Graham, N.T., Ou, Y., Khan, Z., Kholod, N., Narayan, K., Hejazi, M., Kim, S., Calvin, K., Wise, M.: Gcam-usa v5.3_water_dispatch: integrated modeling of subnational us energy, water, and land systems within a global framework. Geoscientific Model Development **15**, 2533–2559 (2022) https://doi.org/10.5194/gmd-15-2533-2022

[43] Licandeo, F., Flores, F., Feijoo, F.: Assessing the impacts of economy-wide emissions policies in the water, energy, and land systems considering water scarcity scenarios. Applied Energy **342**, 121115 (2023) https://doi.org/10.1016/j.apenergy.2023.121115

[44] Waldhoff, S.T., Martinich, J., Sarofim, M., DeAngelo, B., McFarland, J., Jantarasami, L., Shouse, K., Crimmins, A., Ohrel, S., Li, J.: Overview of the special issue: a multi-model framework to achieve consistent evaluation of climate change impacts in the united states. Climatic Change **131**(1), 1–20 (2015) https://doi.org/10.1007/s10584-014-1206-0

[45] Dieter, C.A., Maupin, M.A., Caldwell, R.R., Harris, M.A., Ivahnenko, T.I., Lovelace, J.K., Barber, N.L., Linsey, K.S.: Estimated Use of Water in the United States in 2015 vol. 1441. US Geological Survey, ??? (2018)

[46] Clean Energy States Alliance: Table of 100% Clean Energy States. Accessed: 2024-12-05 (2024). https://www.cesa.org/projects/100-clean-energy-collaborative/guide/table-of-100-clean-energy-states/

[47] Wahid, A., Gelani, S., Ashraf, M., Foolad, M.R.: Heat tolerance in plants: an overview. Environmental and experimental botany **61**(3), 199–223 (2007)

[48] Agriculture, E.R.S.: Farm resource regions. Agricultural Information Bulletin 760, United States Department of Agriculture (2000). Accessed: 2024-12-04. https://www.ers.usda.gov/webdocs/publications/42298/32489_aib-760_002.pdf

[49] Warziniack, T., Arabi, M., Froemke, P., Ghosh, R., Heidari, H., Rasmussen, S., Swartzentruber, R.: Water resources. In: Agriculture, F.S. (ed.) Future of America's Forest and Rangelands: Forest Service 2020 Resources Planning Act Assessment. Gen. Tech. Rep. WO-102, pp. 9–1920. U.S. Department of Agriculture, Forest Service, Washington, DC (2023). Chap. 9. https://doi.org/10.2737/WO-GTR-102-Chap9

[50] Lauer, S., Sanderson, M., Manning, D., Suter, J., Hrozencik, R.A., Guerrero, B., Golden, B.: Values and groundwater management in the ogallala aquifer region. Journal of Soil and Water

Conservation **73**(5), 593–600 (2018)

[51] Bruno, E.M., Hagerty, N., Wardle, A.R.: The political economy of groundwater management: Descriptive evidence from california. American Agriculture, Water Resources, and Climate Change, ed. Gary D. Libecap and Ariel Dinar. University of Chicago Press, forthcoming (2022)

[52] Hoekema, D.J., Ryu, J., Abatzoglou, J.T.: Validation of the impacts of recent aquifer management on the eastern snake plain aquifer in idaho, usa. Groundwater **63**(3), 387–398 (2025)

[53] Agriculture, E.R.S.: Irrigated agricultural acreage has grown, shifting eastward, while western irrigated acreage has declined. https://www.ers.usda.gov/data-products/chart-gallery/gallery/chart-detail/?chartId=107509. Accessed: 2024-10-03 (2023)

[54] USDA Natural Resources Conservation Service: Environmental Quality Incentives Program (EQIP) (2024). https://www.nrcs.usda.gov/programs-initiatives/environmental-quality-incentives-program

[55] U.S. Environmental Protection Agency: Cooling Water Intake Structures (Clean Water Act Section 316(b)) (2014). https://www.epa.gov/cooling-water-intakes

[56] U.S. Department of Energy: Trump Administration Keeps Colorado Coal Plant Open to Ensure Affordable, Reliable and Secure Power in Colorado. Press release (2026). https://www.energy.gov/articles/trump-administration-keeps-colorado-coal-plant-open-ensure-affordable-reliable-and-secure

[57] Mytton, D.: Data centre water consumption. npj Clean Water **4**(1), 11 (2021)

[58] U.S. Department of Energy: 9 Key Takeaways from President Trump's Executive Orders on Nuclear Energy. U.S. Department of Energy Office of Nuclear Energy article (2025). https://www.energy.gov/ne/articles/9-key-takeaways-president-trumps-executive-orders-nuclear-energy

[59] Luukkonen, C.L., Alzraiee, A.H., Larsen, J.D., Martin, D.J., Herbert, D.M., Buchwald, C.A., Houston, N.A., Valseth, K.J., Paulinski, S., Miller, L.D., Niswonger, R.G., Stewart, J.S., Dieter, C.A., Miller, O.L.: Public supply water use reanalysis for the 2000-2020 period by HUC12, month, and year for the conterminous United States (ver. 2.0, August 2024). U.S. Geological Survey data release (2023). https://doi.org/10.5066/P9FUL880

[60] Haynes, J.V., Read, A.L., Chan, A.Y., Martin, D.J., Regan, R.S., Henson, W.R., Niswonger,

R.G., Stewart, J.S.: Monthly crop irrigation withdrawals and efficiencies by HUC12 watershed for years 2000-2020 within the conterminous United States (ver. 2.0, September 2024). U.S. Geological Survey data release (2023). https://doi.org/10.5066/P9LGISUM

[61] Galanter, A.E., Gorman Sanisaca, L.E., Skinner, K.D., Harris, M.A., Diehl, T.H., Lombard, M.A., Chamberlin, C.A., McCarthy, B.A., Halper, A.S., Niswonger, R.G., Stewart, J.S., Markstrom, S.L., Embry, I., Worland, S., Valseth, K.J.: Thermoelectric-power water use reanalysis for the 2008-2020 period by power plant, month, and year for the conterminous United States. U.S. Geological Survey data release (2023). https://doi.org/10.5066/P9ZE2FVM

[62] Thornton, M.M., Shrestha, R., Wei, Y., Thornton, P.E., Kao, S.-C.: Daymet: Daily Surface Weather Data on a 1-km Grid for North America, Version 4 R1. ORNL DAAC, Oak Ridge, Tennessee, USA (2022). https://doi.org/10.3334/ORNLDAAC/2129 . https://doi.org/10.3334/ORNLDAAC/2129

[63] Kao, S.-C., Ghimire, G.R., Gangrade, S.: CMIP6-based Multi-model Streamflow Projections over the Conterminous US, Version 1.1. HydroSource. Oak Ridge National Laboratory, Oak Ridge, Tennessee, USA (2024). https://doi.org/10.13139/OLCF/2318650

[64] Economic Analysis, U.S.B.: Personal Income by County, Metro, and Other Areas. https://www.bea.gov/data/income-saving/personal-income-county-metro-and-other-areas. Accessed: 2024-10-03 (2023)

[65] O'Neill, B.C., Kriegler, E., Ebi, K.L., Kemp-Benedict, E., Riahi, K., Rothman, D.S., Van Ruijven, B.J., Van Vuuren, D.P., Birkmann, J., Kok, K., *et al.*: The roads ahead: Narratives for shared socioeconomic pathways describing world futures in the 21st century. Global environmental change **42**, 169–180 (2017)

[66] Ashfaq, M., Rastogi, D., Kitson, J., Abid, M.A., Kao, S.-C.: Evaluation of cmip6 gcms over the conus for downscaling studies. Journal of Geophysical Research: Atmospheres **127**(21), 2022–036659 (2022)

[67] Rastogi, D., Kao, S.-C., Ashfaq, M.: How may the choice of downscaling techniques and meteorological reference observations affect future hydroclimate projections? Earth's Future **10**(8), 2022–002734 (2022)

[68] Werner, A.T., Cannon, A.J.: Hydrologic extremes–an intercomparison of multiple gridded statistical downscaling methods. Hydrology and Earth System Sciences **20**(4), 1483–1508 (2016)

[69] Wear, D.N., Prestemon, J.P.: Spatiotemporal downscaling of global population and income scenarios for the united states. PloS one **14**(7), 0219242 (2019)

[70] Cameron, A.C., Miller, D.L.: A practitioner's guide to cluster-robust inference. Journal of human resources **50**(2), 317–372 (2015)

[71] Moody, C.E., Marvell, T.B.: Clustering and standard error bias in fixed effects panel data regressions. Journal of Quantitative Criminology **36**, 347–369 (2020)

[72] Newell, R.G., Prest, B.C., Sexton, S.E.: The gdp-temperature relationship: implications for climate change damages. Journal of Environmental Economics and Management **108**, 102445 (2021)

[73] Xie, Y., Hunter, M., Sorensen, A., Nogeire-McRae, T., Murphy, R., Suraci, J.P., Lischka, S., Lark, T.J.: Us farmland under threat of urbanization: Future development scenarios to 2040. Land **12**(3), 574 (2023)

[74] Federal Energy Regulatory Commission: Power Sales and Markets. Accessed: 2024-12-07 (2024). https://www.ferc.gov/power-sales-and-markets

[75] US Department of Energy: National transmission needs study. Technical report, US Department of Energy (December 2023). Accessed: 2023-12-07. https://www.energy.gov/sites/default/files/2023-12/National%20Transmission%20Needs%20Study%20-%20Final_2023.12.1.pdf

[76] Burke, M., Emerick, K.: Adaptation to climate change: Evidence from us agriculture. American Economic Journal: Economic Policy **8**(3), 106–140 (2016)

[77] Kolstad, C.D., Moore, F.C.: Estimating the economic impacts of climate change using weather observations. Review of Environmental Economics and Policy (2020)

[78] Mérel, P., Gammans, M.: Climate econometrics: Can the panel approach account for long-run adaptation? American Journal of Agricultural Economics **103**(4), 1207–1238 (2021)

[79] Raskin, P.D., Hansen, E., Margolis, R.M.: Water and sustainability: Global patterns and long-range problems. In: Natural Resources Forum, vol. 20, pp. 1–15 (1996). Wiley Online Library

[80] Damkjaer, S., Taylor, R.: The measurement of water scarcity: Defining a meaningful indicator. Ambio **46**(5), 513–531 (2017)

[81] Hanasaki, N., Yoshikawa, S., Pokhrel, Y., Kanae, S.: A quantitative investigation of the thresholds for two conventional water scarcity indicators using a state-of-the-art global hydrological

model with human activities. Water Resources Research **54**(10), 8279–8294 (2018)

[82] Rijsberman, F.R.: Water scarcity: fact or fiction? Agricultural water management **80**(1-3), 5–22 (2006)

[83] Hussain, Z., Wang, Z., Wang, J., Yang, H., Arfan, M., Hassan, D., Wang, W., Azam, M.I., Faisal, M.: A comparative appraisal of classical and holistic water scarcity indicators. Water Resources Management **36**(3), 931–950 (2022)

[84] Liu, J., Yang, H., Gosling, S.N., Kummu, M., Flörke, M., Pfister, S., Hanasaki, N., Wada, Y., Zhang, X., Zheng, C., *et al.*: Water scarcity assessments in the past, present, and future. Earth's future **5**(6), 545–559 (2017)

[85] Circle of Blue: Water Pricing - U.S. Municipal Water Rates Dashboard. Accessed: 2024-12-04 (2024). https://www.circleofblue.org/waterpricing/

Appendix A Appendix

A.1 Supplementary analysis

A.1.1 Interdependencies across water use sectors

To test for interdependencies across sectors, we estimate the equations for PU and CI simultaneously using a SUR model to assess the stability and significance of coefficients. In this context, the SUR model jointly estimates the PU (1) and CI (2) equations while allowing the error terms to be correlated across equations, improving efficiency and enabling tests of whether cross-equation correlations materially affect coefficient estimates. The results indicate that key climate coefficients, such as those for temperature, precipitation, and soil moisture, are consistent in magnitude and significance with those from the sector-specific models (Figure Figure A13). For PU, the marginal effects of temperature exhibit minor differences but remain qualitatively similar. Similarly, for CI, the seasonal marginal effects of climate variables align closely with those from the individual models. Notably, the SUR model precludes the two-way clustering of standard errors applied in the sector-specific models, resulting in much tighter confidence intervals. Overall, these findings provide suggestive evidence that any interdependencies across sectors do not meaningfully bias our results, giving us additional confidence in the suitability of our statistical framework for explaining and predicting water use.

A.2 Supplementary tables

Table A1 Summary statistics for annual average water withdrawals by water use category. Units are gallons per person per (GPD) day for public use, and acre-feet per day (AFD) for crop irrigation and thermoelectric power generation. The units of analysis are county for public use and crop irrigation and power plant for thermoelectric power.

Water Use Category	Obs	Mean	Std. Dev.	Min	Median	Max
Public Use (GPD)	3,108	103.74	67.38	0.00	92.98	1,432.28
Crop Irrigation (AFD)	3,108	98.12	387.20	0.00	2.05	9,075.05
Thermoelectric Power (AFD)	2,434					
Biomass	236	8.53	25.11	0.00	0.85	188.53
Coal	838	209.03	460.39	0.00	29.43	4,614.72
Gas	822	36.04	134.31	0.00	2.70	2,405.96
Multi-fuel	381	162.26	402.55	0.00	14.20	4,134.09
Nuclear	116	1,035.86	1,444.31	0.25	158.11	5,384.96
Oil	41	9.43	16.33	0.00	0.47	56.56

Table A2 Summary of data sources

Variable Class	Variables	Source	Spatial Res.	Temporal Res.	Temporal Ext.
Climate (historical)	Precipitation Temperature Wind speed Humidity	Daymet [62]	4 km	Daily	2000-2020
Climate (projected)	*	CMIP6 [63]	4km	Daily	2025-2100
Hydrology	Runoff SWE Soil moisture	VIC [63]	4 km	Daily	2000-2100
Population (historical)	Population	BEA [64]	County	Annual	1969-2022
Population (projected)	Population	[69]	County	5-year	2010-2070
Water Use (historical)	Public Use [59] Crop Irrigation [60] TEP [61]	USGS	HUC12	Monthly	2000-2020

Table A3 Model fit statistics, variables, interactions, and fixed effects for Public Use, Crop Irrigation, and Thermoelectric Power Generation models.

	Public Use	**Crop Irrigation**	**TP Generation**
Variables			
Max temperature	✓	✓	✓
Precipitation	✓	✓	–
Humidity	✓	✓	✓
Runoff	✓	✓	✓
Soil moisture	✓	✓	–
Wind speed	✓	✓	✓
Population	–	✓	✓
County time trends	✓	✓	–
Interactions			
Seasonal	✓	✓	✓
ERS FRR	–	✓	–
Cooling technology	–	–	✓
Fixed effects			
County-month (37,296)	✓	✓	–
State-year (960)	✓	✓	–
Plant-month (29,208)	–	–	✓
ISO-year (200)	–	–	✓
Fit statistics			
Observations	745,920	745,920	238,272
Log-likelihood	-2,660,758	-3,764,931	-1,264,477
AIC	5,404,427	7,613,926	2,587,158
BIC	5,882,087	8,098,235	2,889,271
R^2	0.986	0.957	0.937
Pseudo R^2	0.375	0.238	0.206
Adjusted R^2	0.985	0.954	0.928
Within adjusted R^2	0.375	0.136	0.011
Wald	$7.39 \times 10^{9***}$	$2.65 \times 10^{10***}$	518.5^{***}
F-test	134.6^{***}	30.7^{***}	17.0^{***}

Notes: Standard errors are clustered at the following levels:
PU and CI: County (FIPS) and state-year clusters.
TP: Plant and ISO-year clusters.
*Signif. Codes: ***: 0.01, **: 0.05, *: 0.1*

Table A4 100% clean energy goals by state [46]

State	**Goal**	**Target Year**
California	100% carbon-free electricity	2045
Colorado	100% carbon-free electricity for Xcel Energy	2050
Connecticut	100% carbon-free electricity	2040
District of Columbia	100% renewable energy	2032
Hawaii	100% renewable energy	2045
Louisiana	Net zero greenhouse gas emissions	2050
Maine	100% clean energy	2050
Massachusetts	Net-zero greenhouse gas emissions	2050
Michigan	100% clean energy	2040
Minnesota	100% carbon-free electricity	2040
Nebraska	Net-zero carbon emissions from public power utilities	2050
Nevada	100% carbon-free energy	2050
New Jersey	100% clean energy	2050
New Mexico	100% zero-carbon electricity	2045
New York	100% carbon-free electricity	2040
North Carolina	Net-zero greenhouse gas emissions	2050
Oregon	100% clean electricity	2040
Puerto Rico	100% renewable energy	2050
Rhode Island	100% renewable electricity	2033
Virginia	100% carbon-free electricity	2045
Washington	100% clean electricity	2045
Wisconsin	100% carbon-free electricity	2050

A.3 Supplementary figures

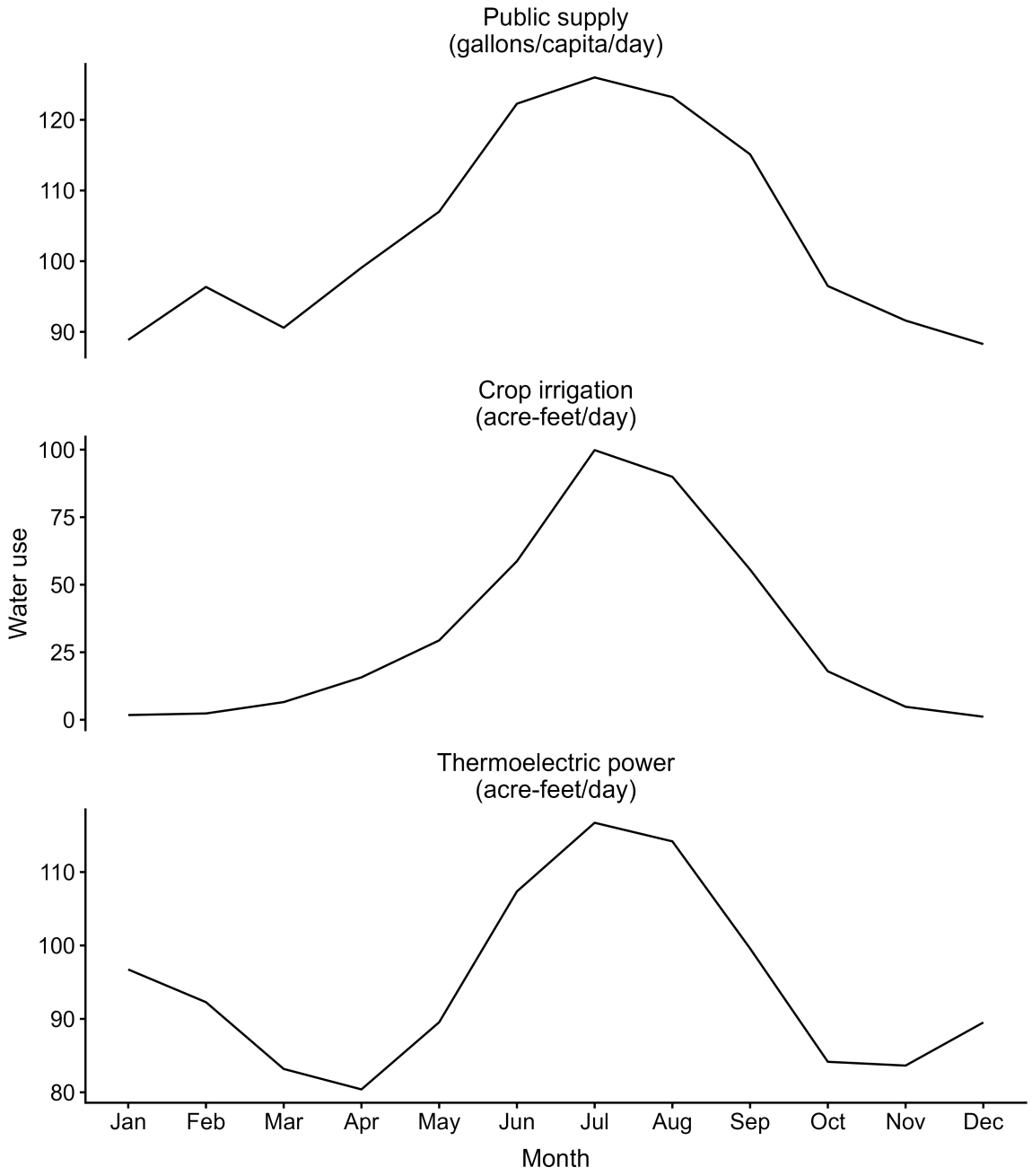


Fig. A1 Seasonal patterns in average water use across major sectors in the conterminous United States. Values represent monthly averages across all counties and years in the historical sample (2000–2020).

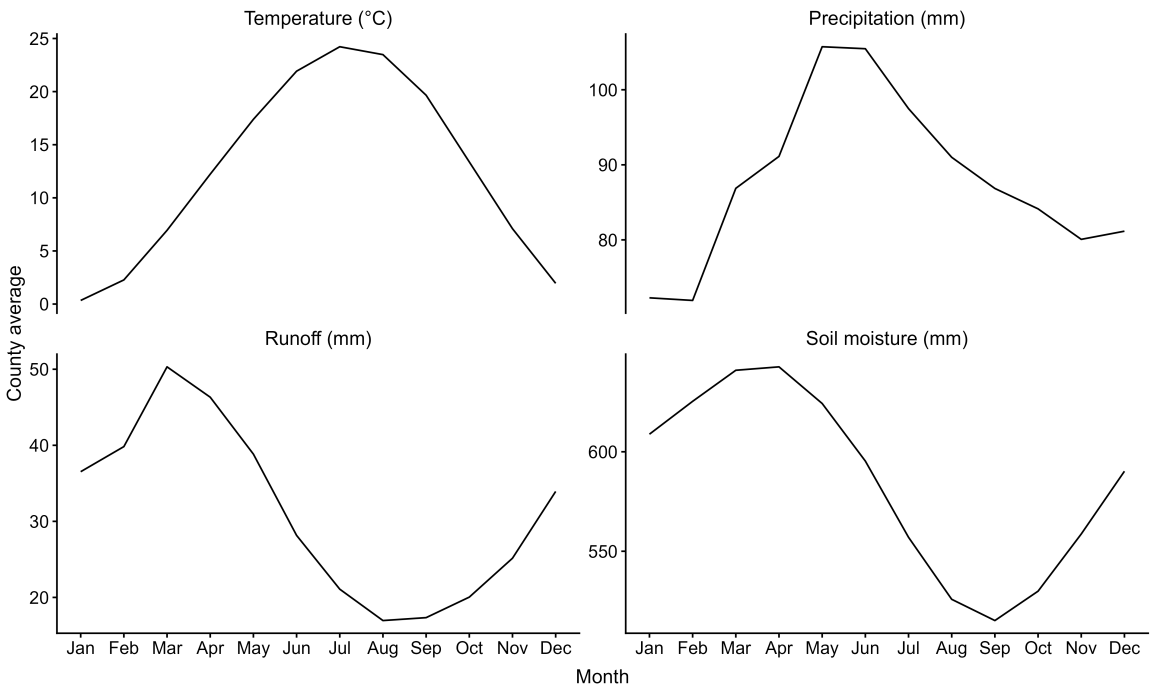


Fig. A2 Seasonal patterns in key hydroclimatic variables across the conterminous United States. Values represent monthly averages across all counties and years in the historical sample (2000–2020).

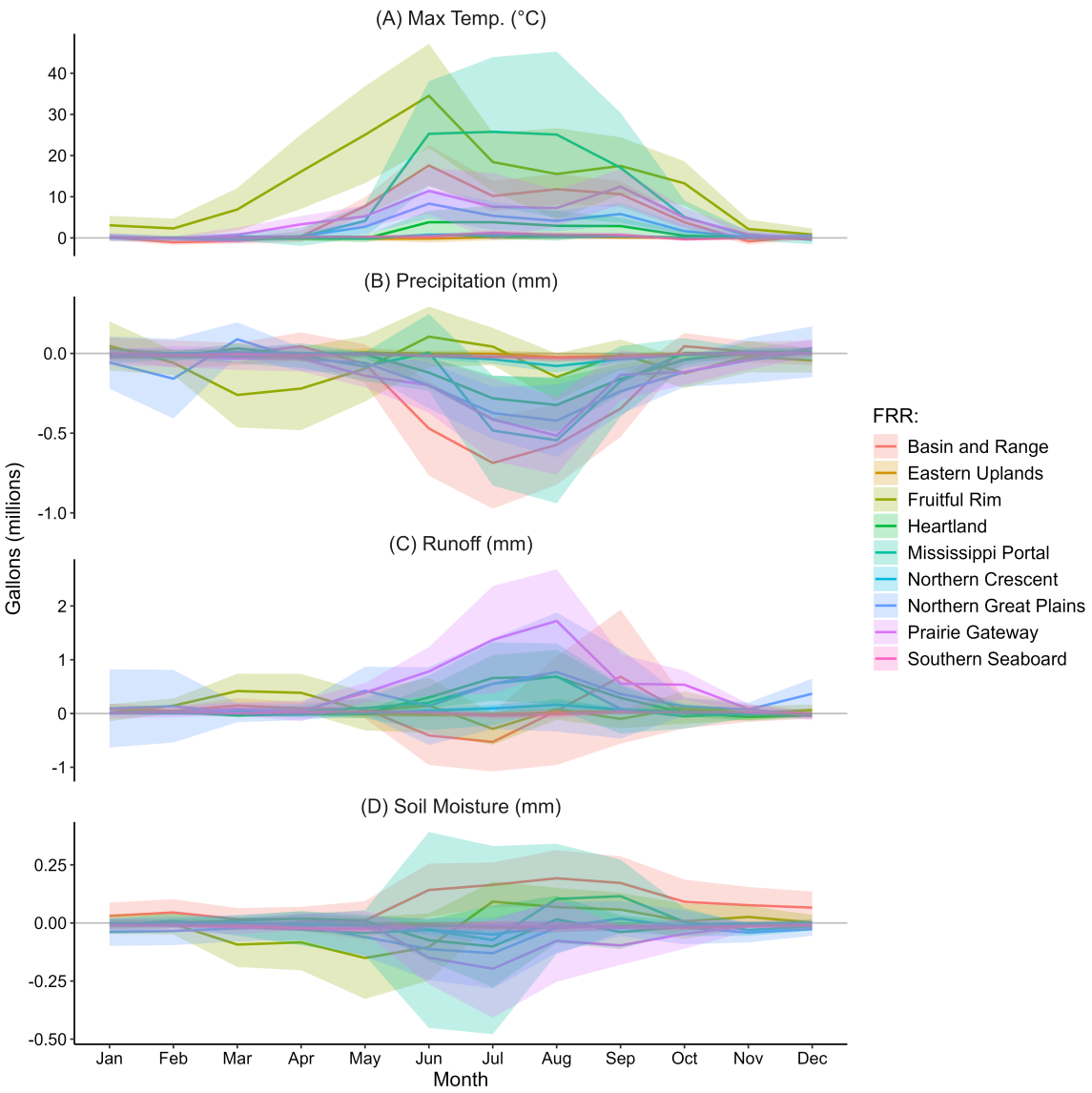


Fig. A3 Estimated seasonal marginal effects of the impacts of climate and hydrology on water withdrawals for crop irrigation by ERS farm resource region. Confidence intervals are at the 95% level.

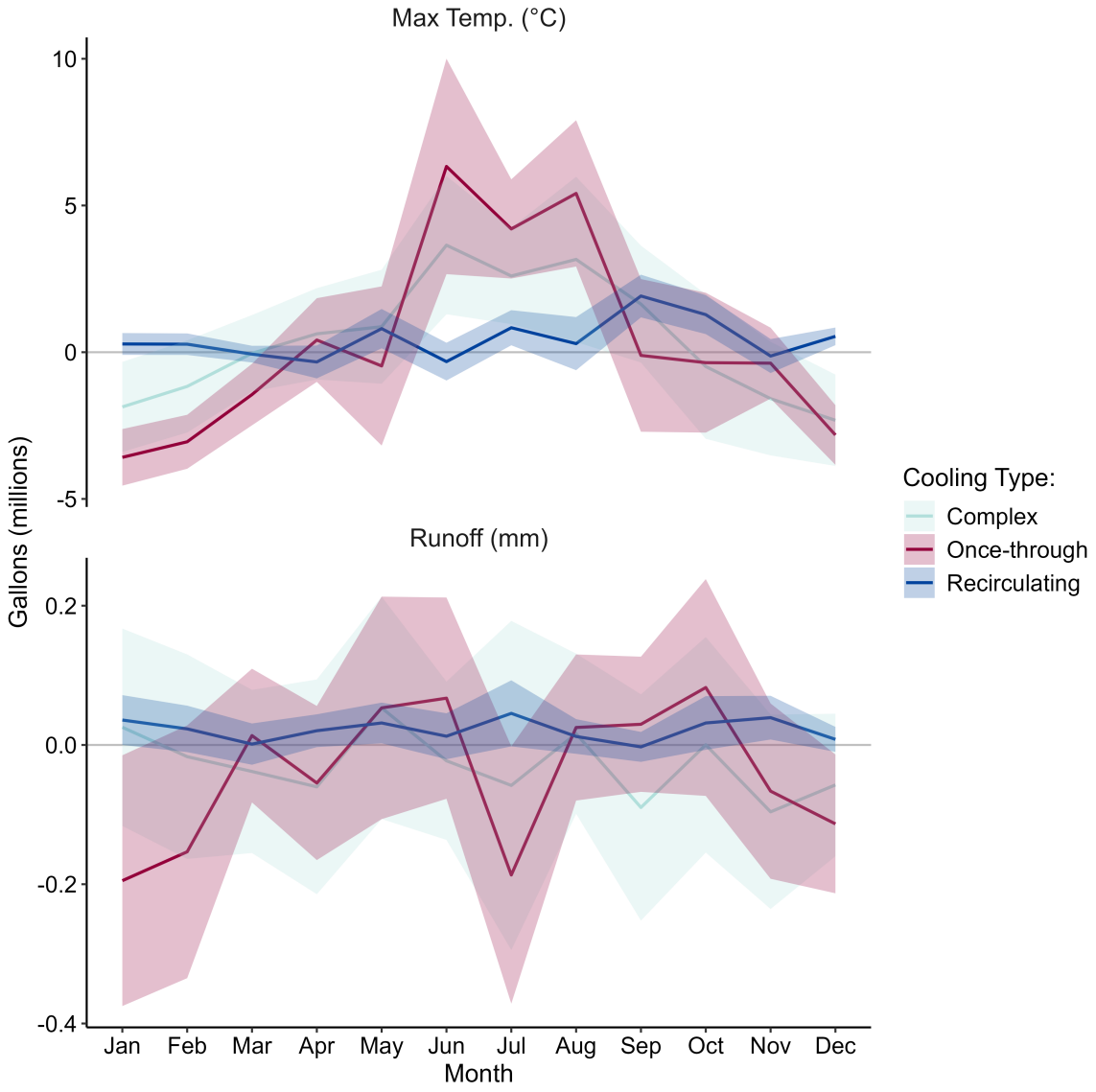


Fig. A4 Estimated seasonal marginal effects of the impacts of climate and hydrology on water withdrawals for thermoelectric power generation by plant cooling technology. Confidence intervals are at the 95% level.

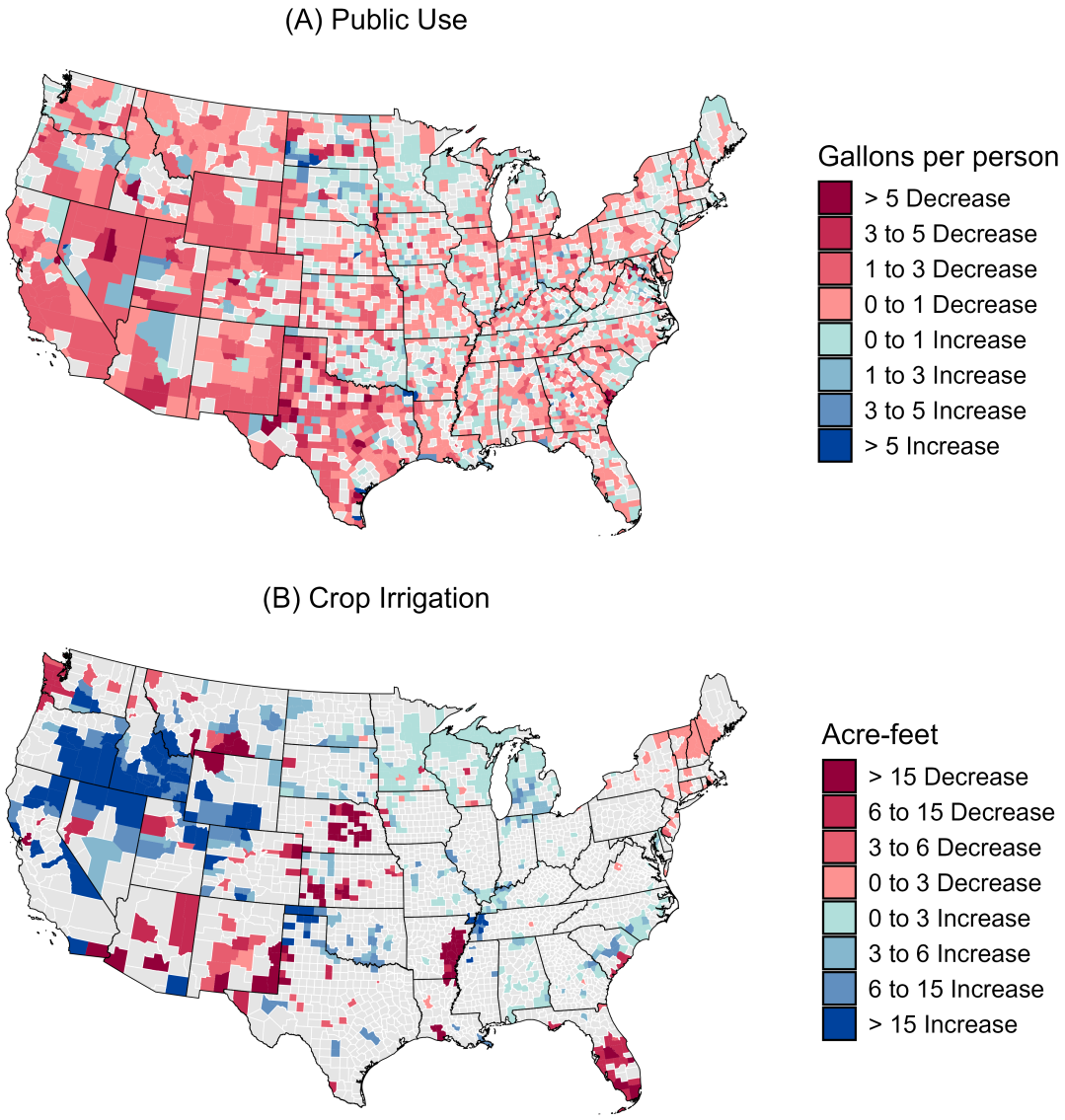


Fig. A5 Statistically significant annual water use trends ($\alpha = 0.05$) for public use and crop irrigation after controlling for climate, population, and unobserved confounding variables.

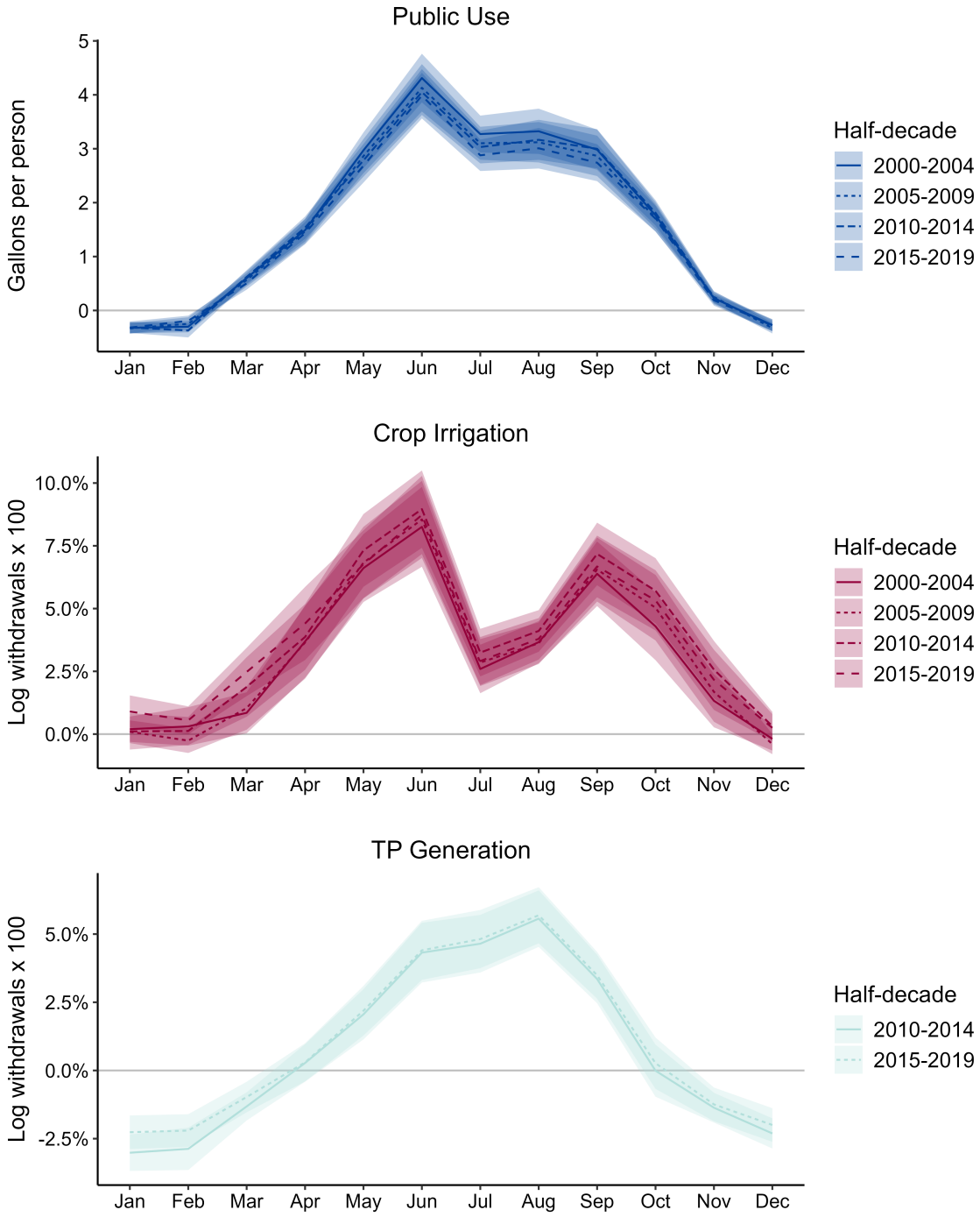


Fig. A6 Seasonal marginal effects of temperature on water withdrawals by half-decade time step.

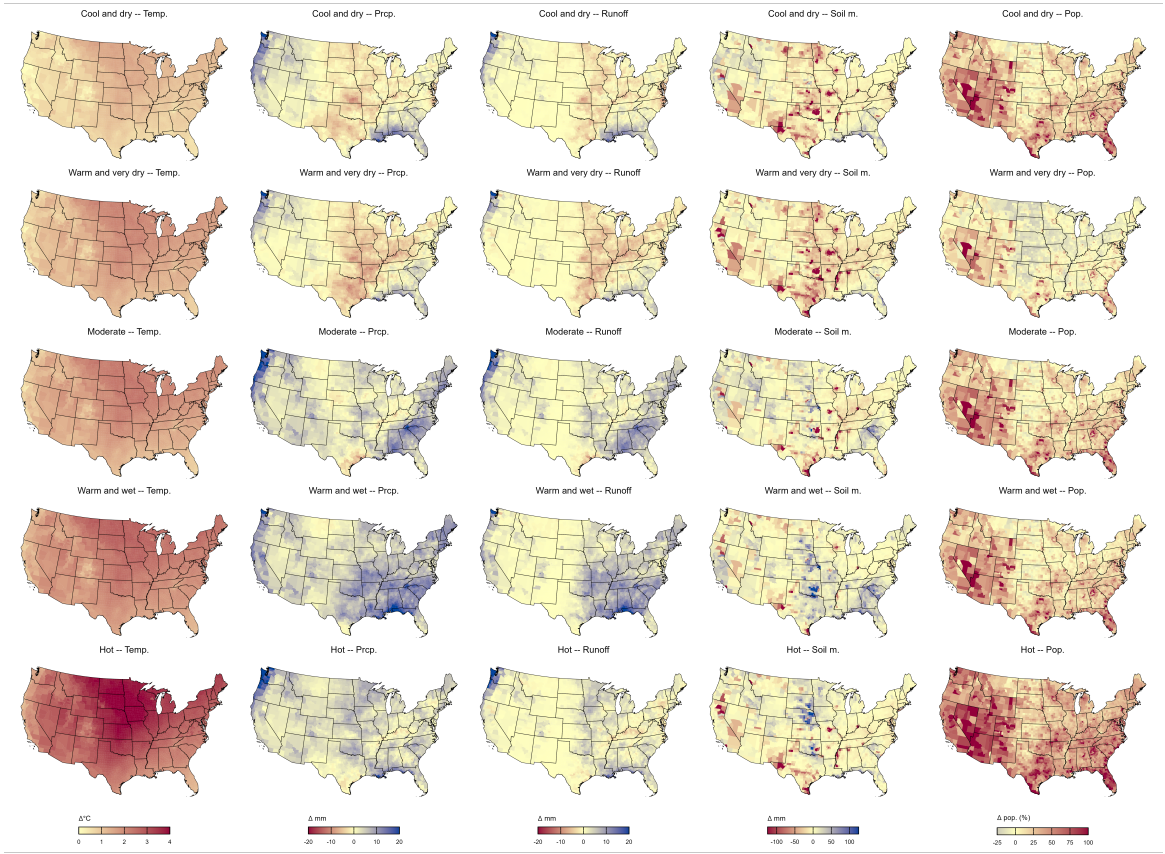


Fig. A7 Spatial distribution of projected changes in climate and population across five stylized scenarios (2040–2070 relative to 2000–2020). Rows correspond to scenarios (Cool and dry, Warm and very dry, Moderate, Warm and wet, and Hot), while columns show changes in temperature, precipitation, runoff, soil moisture, and population. Values represent county-level averages.

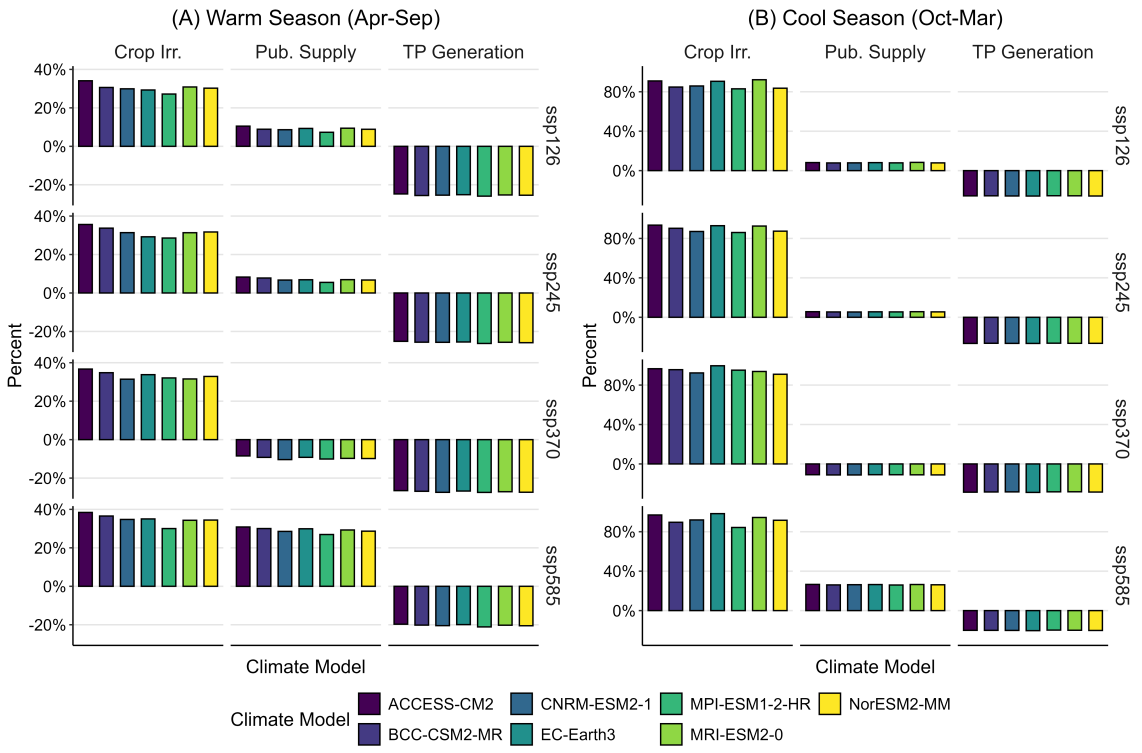


Fig. A8 Total future percent changes in water withdrawals by water use category, season, climate model, and emission scenario.

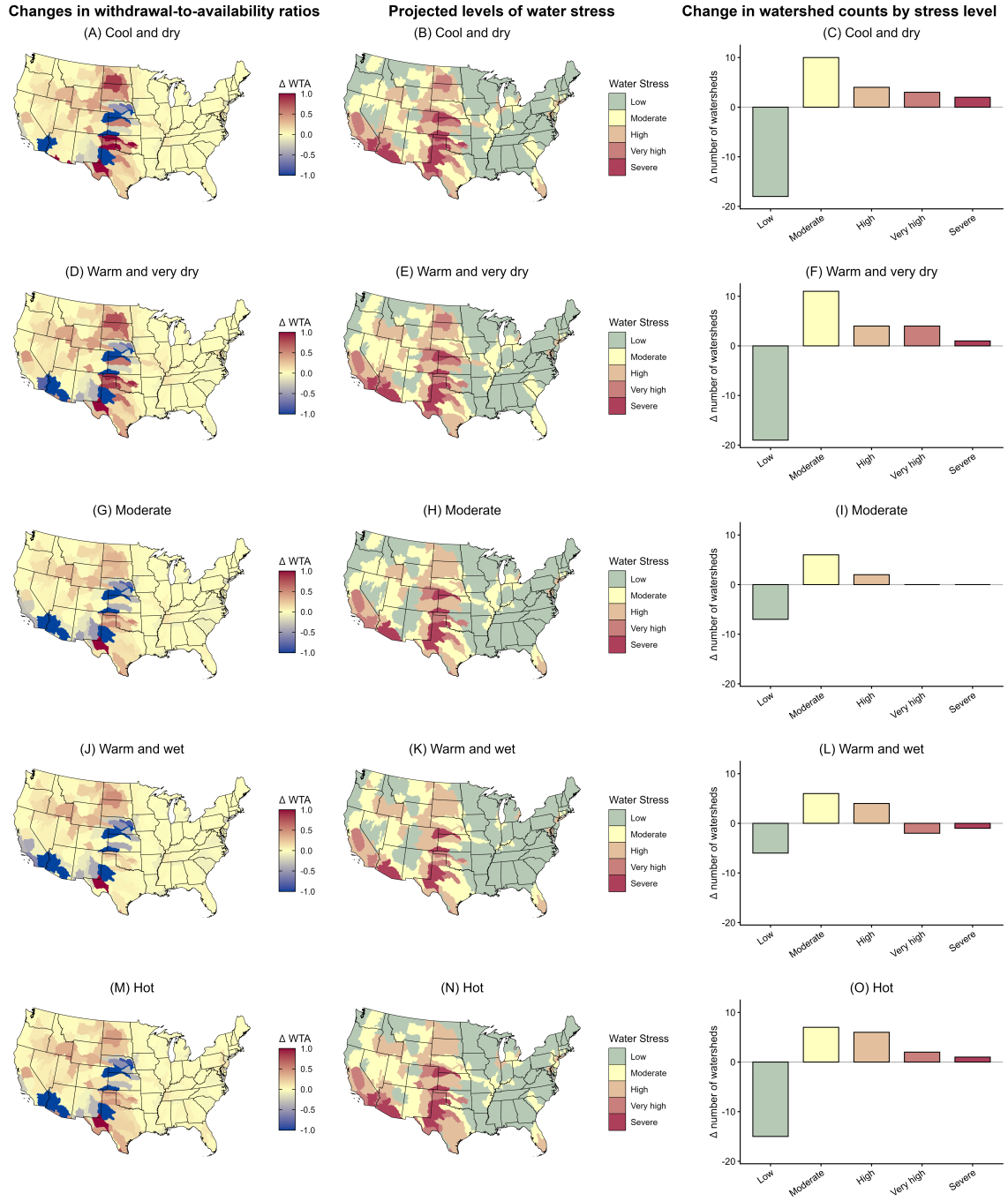


Fig. A9 Projected changes in water scarcity across stylized climate–population scenarios (2040–2070 relative to 2000–2020) by HUC04 subregion. For each scenario, panels in the left column show changes in withdrawal-to-availability (WTA) ratios, panels in the middle column display projected water stress categories, and panels in the right column summarize changes in the number of watersheds by stress level. Positive (negative) values in WTA indicate increasing (decreasing) water stress.

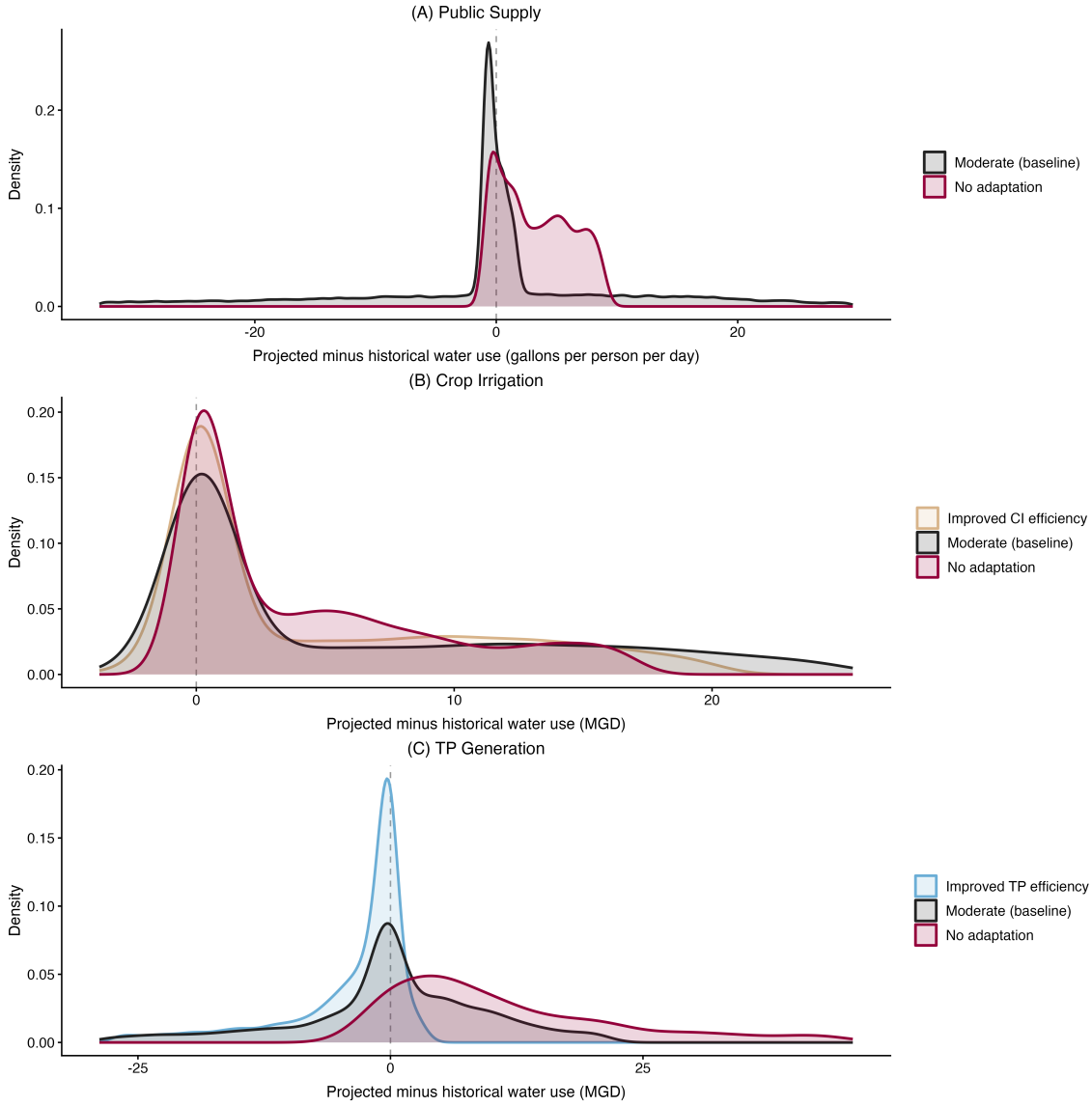


Fig. A10 Distributions of projected changes in water use (2040–2070 relative to 2000–2020) under alternative counterfactual scenarios for (A) public supply, (B) crop irrigation, and (C) thermoelectric power generation across all counties. Changes are shown as projected minus historical withdrawals, with vertical dashed lines indicating no change.

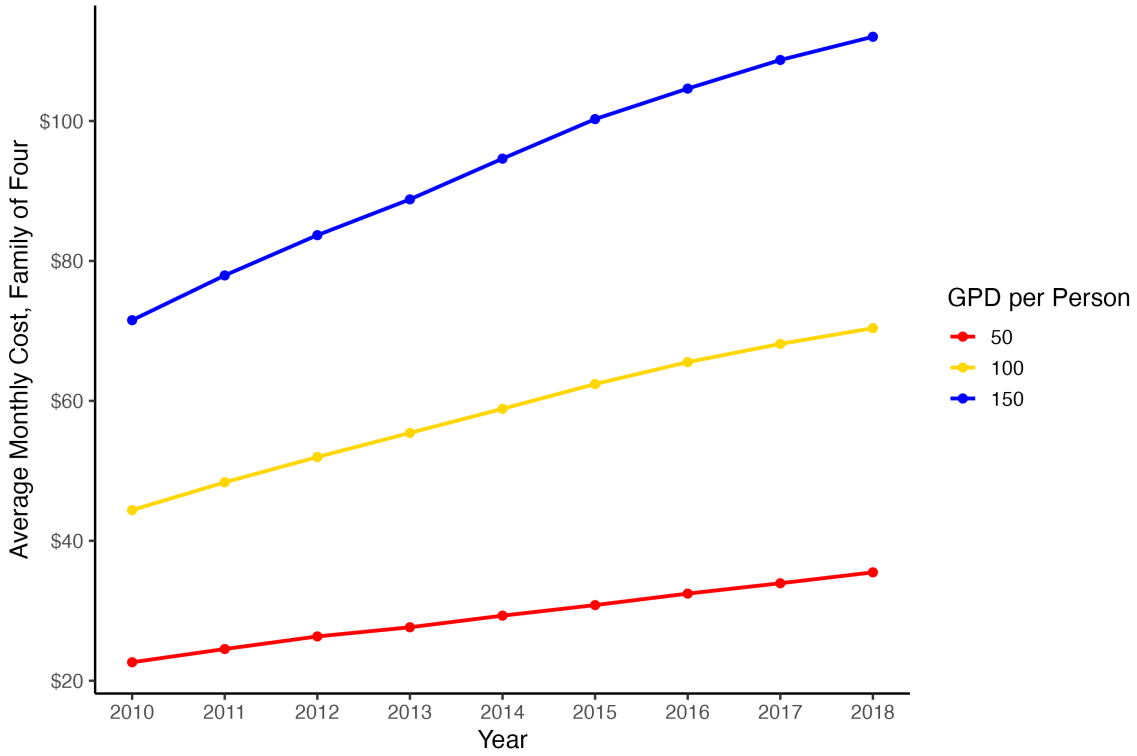


Fig. A11 Average water prices from 30 major US cities by household type [85]

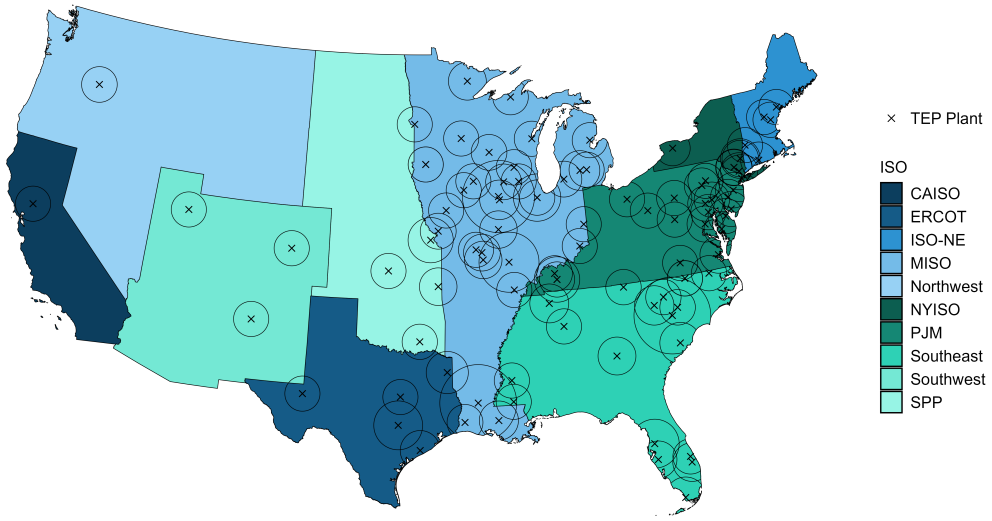


Fig. A12 US map of ISOs and example transmission constraints for 100 randomly sampled power plants

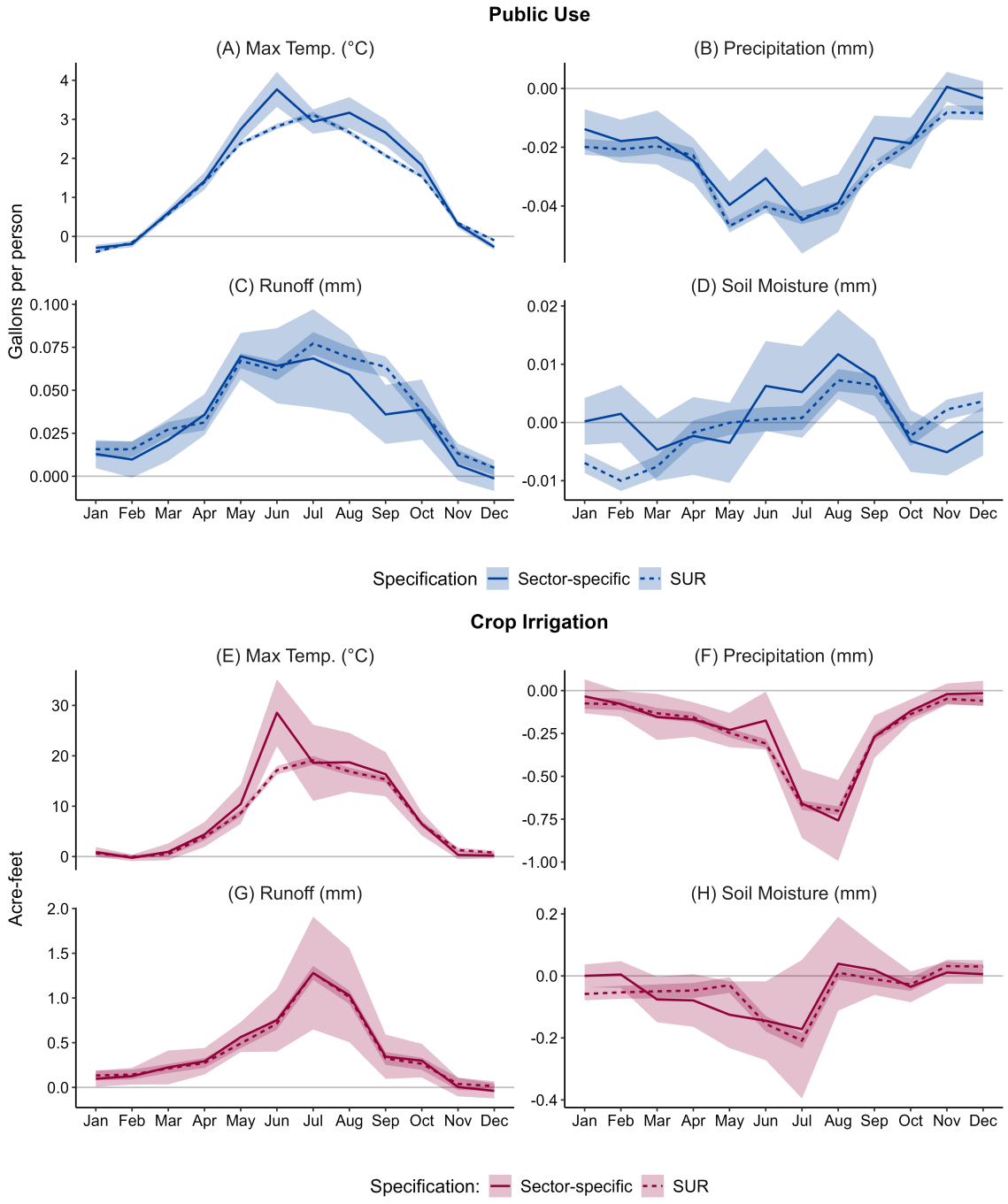


Fig. A13 Comparison of seasonal marginal effects between sector-specific models and SUR

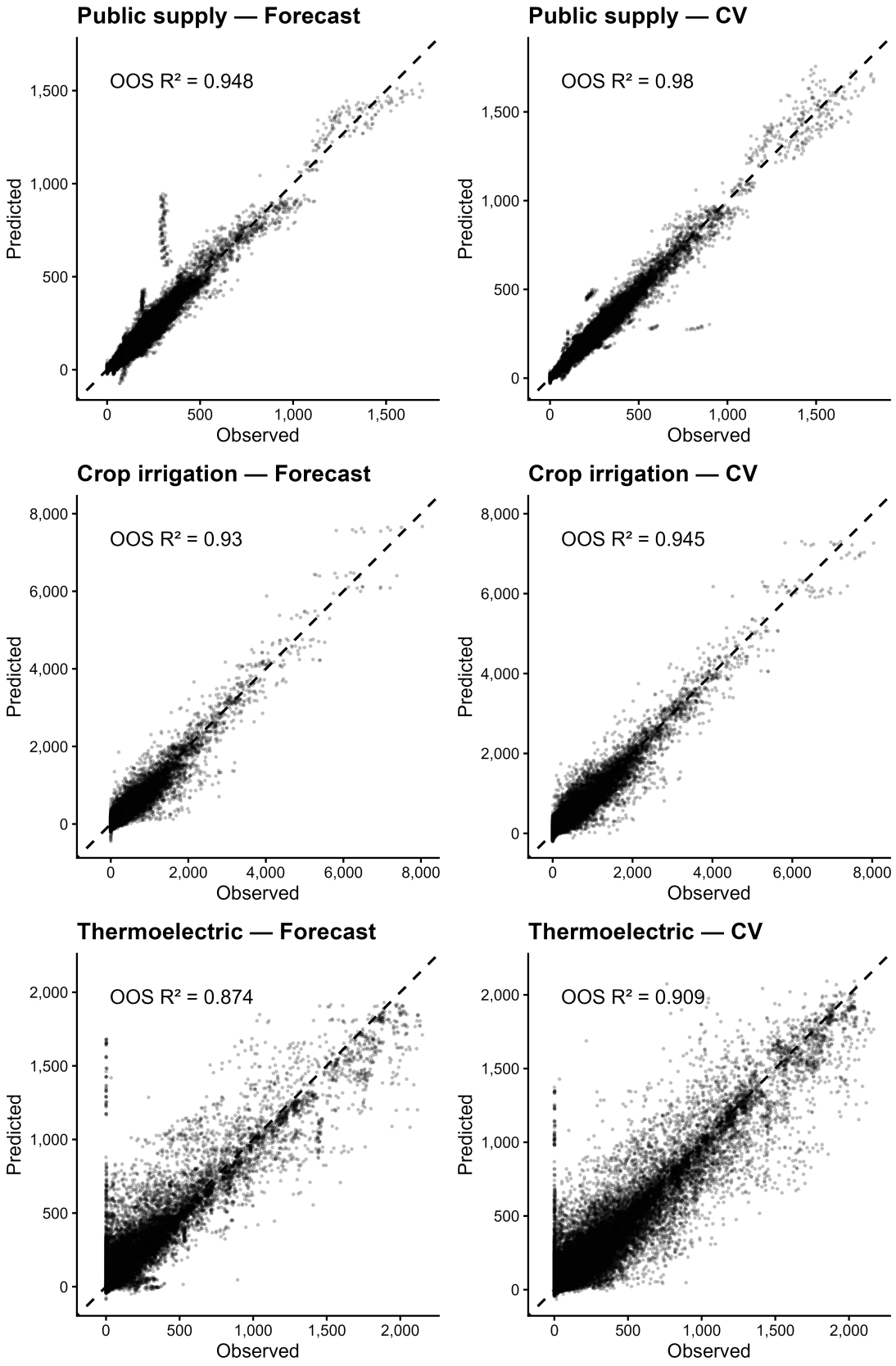


Fig. A14 Out-of-sample validation of sector-specific water use models. Points show observed versus predicted monthly withdrawals under (left column) forecast splits and (right column) temporally structured cross-validation. Dashed lines indicate the 45-degree line. Reported values are out-of-sample R^2.